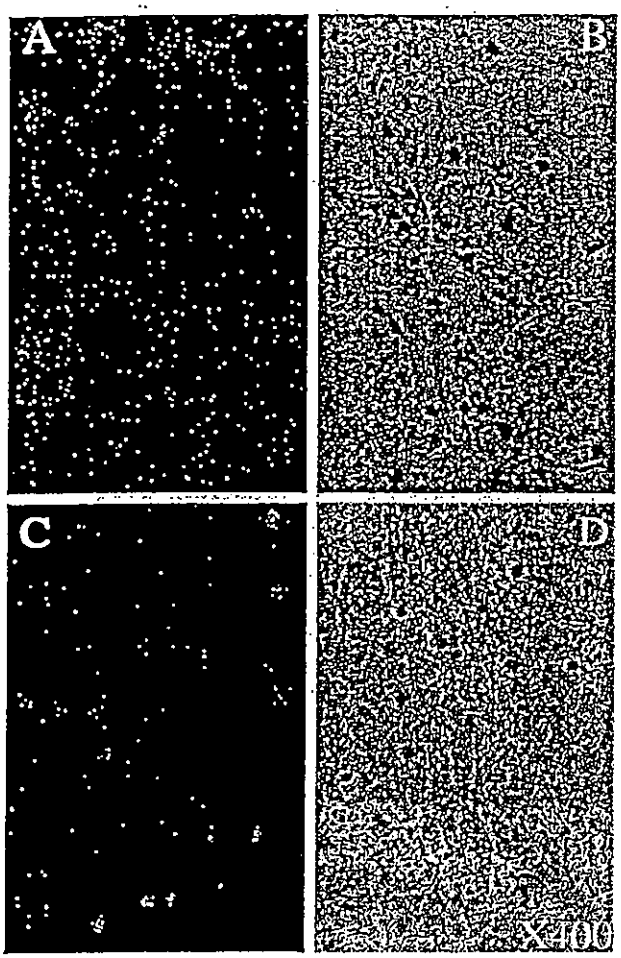

Fig. 2. A fluorescence micrograph of the rat liver (**A**) (×400) and hematoxylin and eosin staining of the same section (**B**) (×400) 1 h after the intraportal injection of HVJ anionic liposomes containing FITC-ODN. Fluorescent signals were detected mainly in the nuclei of hepatocytes and no hepatotoxicity was detected either histologically or serologically. Similar results were obtained in the sections 24 h after the injection, as shown in (**C**) and (**D**).

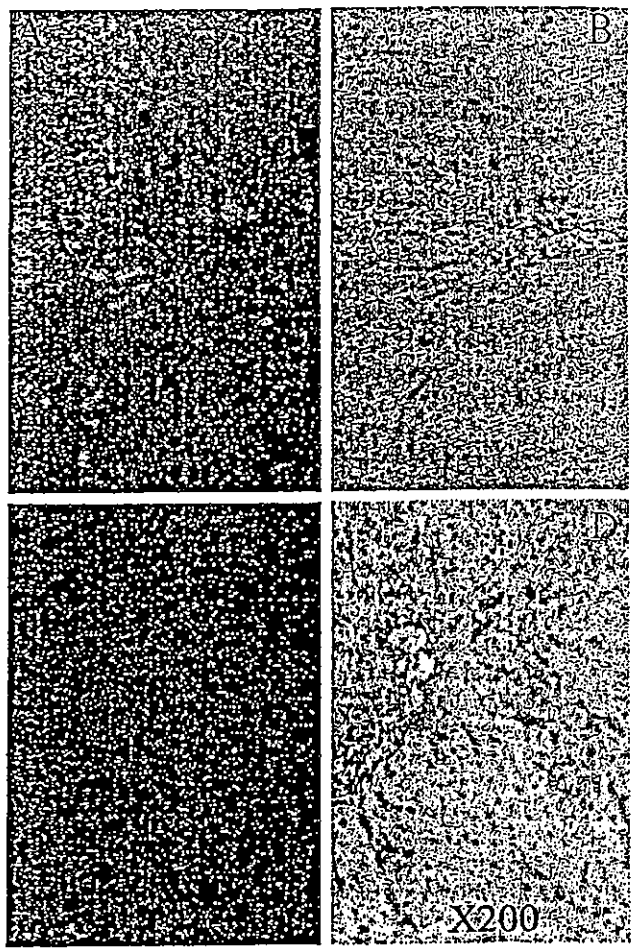

Fig. 3. A fluorescence micrograph of the rat liver (**A**) (×200) and immunohistochemical staining of the same section with monoclonal antibody to tissue macrophage specific glycoprotein (**B**) (×200) 1 h after the intraportal injection of HVJ cationic liposome containing FITC-ODN. Fluorescent signals were detected in approximately 90% of macrophage-specific glycoprotein-positive Kupffer cells. No hepatotoxicity was detected either histologically or serologically. Similar results were obtained in the sections 24 h after the injection, as shown in (**C**) and (**D**).

ciency 24 h after the intravenous injection was slightly improved but still much lower than that by portal injection (fig. 4C, D). The transfection efficiency of FITC-ODN to Kupffer cells at 1 h and 24 h after injection of the HVJ cationic liposomes is shown in table 1. No histological damage was detected in hepatocytes or nonparenchymal cells using either HVJ anionic or HVJ cationic liposome methods, as indicated by the plasma levels of AST and ALT 24 h after the injection of BBS, HVJ anionic liposomes and HVJ cationic liposomes via the portal vein (table 2). A slight elevation of AST and ALT was observed even in rats injected with BBS, probably due to clamping the portal vein for 15 min. There were no significant differences in plasma levels of either AST or ALT among rats injected with BBS, HVJ anionic liposomes and HVJ cationic liposomes.

Transfection Efficiency and Localization after Injection of Conventional Cationic Liposomes without HVJ Intravenously or Intraportally in vivo

One hour after intravenous cationic liposome injection only a few fluorescent signals were detected in the cells

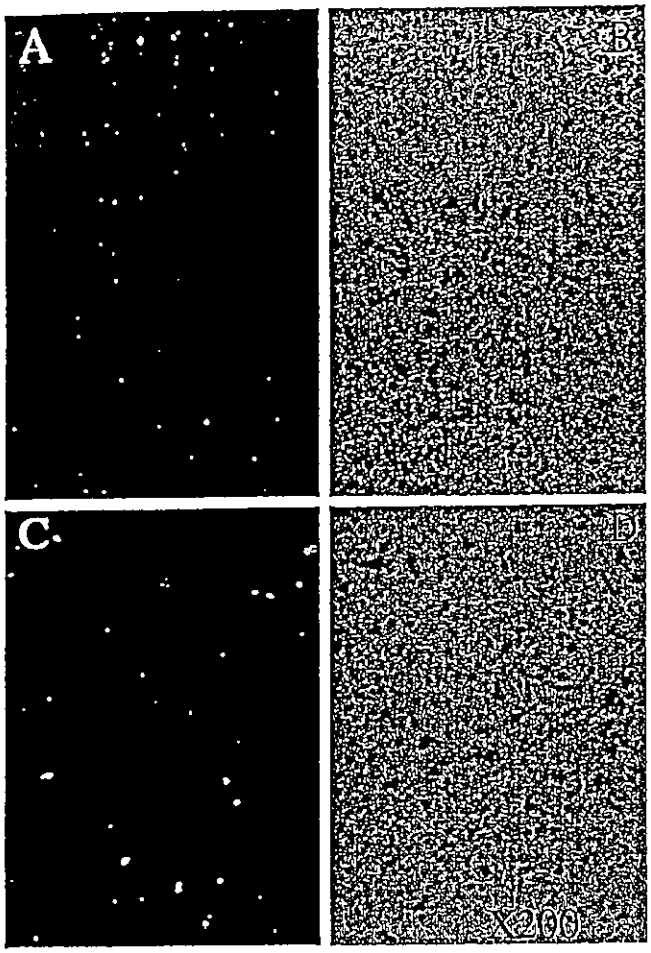

Fig. 4. A fluorescence micrograph of the rat liver (A) (×200) and immunohistochemical staining of the same section with monoclonal antibody to tissue macrophage specific glycoprotein (B) (×200) 1 h after the intravenous injection of HVJ cationic liposome containing FITC-ODN via the tail vein. Only a few fluorescent signals were detected in the cells that were immunohistochemically identified as Kupffer cells. In the sections of 24 h after the injection, as shown in (C) and (D), more fluorescent signals were detected in Kupffer cells than at 1 h after the injection, but the number was much lower than that after transfection of HVJ cationic liposomes.

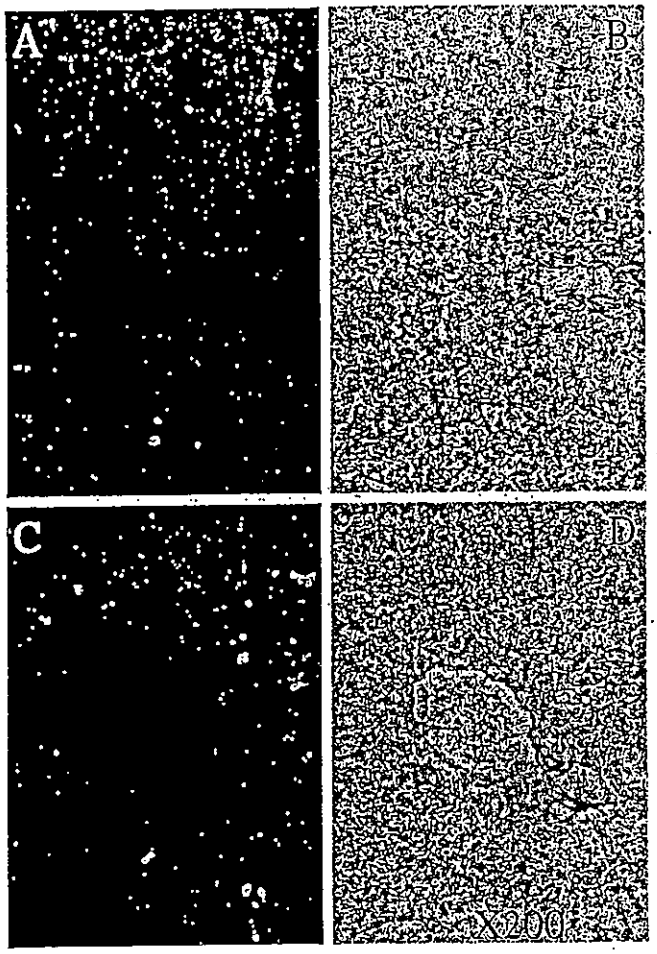

Fig. 5. A fluorescence micrograph of the rat liver (A) (×200) and immunohistochemical staining of the same section with monoclonal antibody to tissue macrophage-specific glycoprotein (B) (×200) 1 h after the intravenous injection of conventional cationic liposome without HVJ containing FITC-ODNs via the tail vein. Only a few fluorescent signals were detected in the cells that were immunohistochemically identified as Kupffer cells. In the sections of 24 h after the injection, as shown in (C) and (D), more fluorescent signals were detected in Kupffer cells than at 1 h after the injection, but the number was much lower than that after transfection of HVJ cationic liposomes.

Table 1. Transfection efficiency of FITC-labeled oligonucleotide into Kupffer cells

	1 h after		24 h after	
Injection of HVJ cationic liposome via portal vein	85±9.6%	$p<0.01$	90±13.2%	$p<0.01$
Injection of HVJ cationic liposome via tail vein	3.7±3.2%	$p<0.01$	15±4.7%	$p<0.01$
Injection of cationic liposome via portal vein	8.2±2.5%	$p<0.01$	28±8.8%	$p<0.01$
Injection of cationic liposome via tail vein	2.2±1.8%		25±6.6%	

The transfection efficiency of FITC-labeled oligonucleotide in HVJ cationic liposomes injected via the portal vein was significantly better than that in HVJ cationic liposomes injected via the tail vein or that in cationic liposomes without HVJ injected via either the portal vein or tail vein both 1 and 24 h after injection. The data were expressed as mean ± SEs (n = 6 for each group).

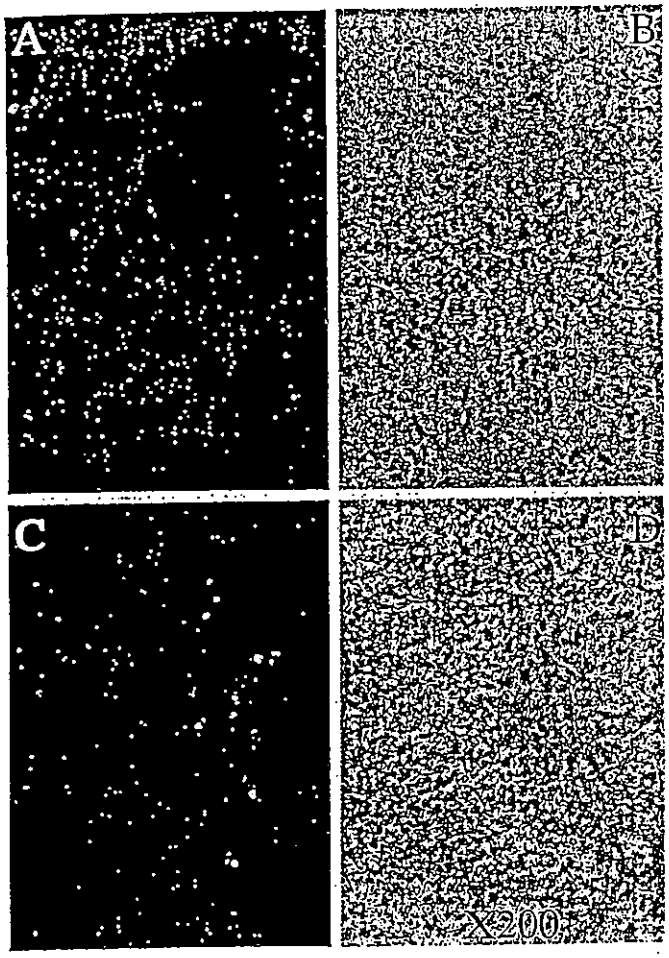

Table 2. The plasma levels of AST and ALT 24 h after the injection

	AST, IU/l	ALT, IU/l
BSS (n = 3)	323±101	162±62.2
HVJ anionic liposome (n = 3)	295±209	91.7±45.7
HVJ cationic liposome (n = 3)	165±94.7	92.0±52.8

The plasma levels of AST and ALT 24 h after the injection of balanced saline solution (BBS), HVJ anionic liposome and HVJ cationic liposome via portal vein in rats. The data were expressed as mean ± SEs. No significant differences were detected by Student's t test.

Fig. 6. A fluorescence micrograph of the rat liver (**A**) (×200) and immunohistochemical staining of the same section with monoclonal antibody to tissue macrophage specific glycoprotein (**B**) (×200) 1 h after the intraportal injection of conventional cationic liposomes containing FITC-ODN with clamping of the portal vein for 15 min. Only a few fluorescent signals were detected in the cells that were immunohistochemically identified as Kupffer cells and the transfection efficiency was as low as that after intravenous injection. No improvement was obtained by using portal injection. In the sections of 24 h after the injection, as shown in (**C**) and (**D**), moderate improvement in the transfection efficiency was observed in comparison with that 1 h after injection. The efficiency is, however, even much lower than that after injection of HVJ liposomes.

Fig. 7. Light micrographs showing β-galactosidase staining after intraportal injection of expression vector (pCAG-lacZ) in HVJ cationic liposomes containing HMG-1 (**A**). Rats were sacrificed 3 days after transfection of the lacZ gene. No parenchymal cells of the liver were stained, while sinusoidal lining cells, which were thought to be Kupffer cells by the immunohistochemistry in the serial section (**B**), were selectively stained with X-gal.

that were immunohistochemically identified as Kupffer cells (fig. 5A, B). More fluorescent signals were detected in Kupffer cells 24 h after the injection (fig. 5C, D), but the numbers were much lower than those after transfection of HVJ cationic liposomes (table 1). The transfection efficiency 1 h (fig. 6A, B) and 24 h (fig. 6C, D) after intraportal injection of cationic liposomes was as low as that after intravenous injection (table 1).

The Localization of pCAG-lacZ Expression

No parenchymal cells of the liver were stained while sinusoidal lining cells which were thought to be the Kupffer cells by the immunohistochemistry in the serial section were selectively stained with X-gal after intraportal injection of HVJ cationic liposomes containing HMG-1 and pCAG-lacZ expression plasmid (fig. 7).

Discussion

In this study, we have demonstrated efficient gene transfer to Kupffer cells using HVJ cationic liposomes for the first time.

Initially, we performed an in vitro study to determine the minimum incubation time necessary for transfection of the liposomes into the cells, since lengthy portal clamping is harmful to the liver. The liposomes containing FITC-ODN were effectively transfected into NR8383 cells within minutes. In the in vivo study, FITC-ODN was detected in approximately 90% of the Kupffer cells when transfected with HVJ cationic liposomes, while FITC-ODN was mainly present in hepatocytes when transfected with HVJ anionic liposomes. The difference in cellular localization appears to be due to the influence of several factors. One important factor is likely to be the size and charge of the liposomes. The liver capillary or sinusoid is different from capillaries in other organs in that it has fenestrations of about 0.2 μm in diameter [21]. Liposomes of small size are mainly transferred into hepatocytes because they can pass through the fenestrations, while larger liposomes are mainly transferred into Kupffer cells and some endothelial cells [16, 17]. The diameter of both HVJ cationic and HVJ anionic liposomes in this study was 0.2 μm, which should allow passage through the fenestrations to reach hepatocytes. Judging from our results, the HVJ cationic liposomes appear to be attracted electrostatically to the negatively charged Kupffer cells lining the sinusoidal surface and to fuse to the cell membrane and therefore to become unable to pass through the fenestrations.

Several mechanisms are reportedly involved in the transfer of liposomes without HVJ into Kupffer cells. One mechanism involves phagocytosis. The cationic liposomes interact with the negatively charged serum opsonin. The complex of the liposomes and opsonin becomes a large electroneutral particle that is phagocytosed by Kupffer cells, after which the liposome is subject to lysosomal digestion and does not reach the nuclei [18]. Another mechanism involves receptor-mediated transfer. There are glycotrophic receptors on the surfaces of Kupffer cells and hepatocytes. The glycosylated liposomes are endocytosed via these receptors by Kupffer cells or hepatocytes. Which type of cell incorporates the liposomes depends on the glycosylated lipids in the liposomes [19]. In this mechanism, the uptake of liposomes by these cells should be limited due to the saturation of receptors resulting in insufficient transfection [22]. Neither phagocytosis nor receptor-mediated transfer appeared to be involved in our study, since the FITC-ODN was transferred mainly into the cell nuclei in a dose-dependent fashion (data not shown). In this study, it appears likely that HVJ cationic liposomes were attracted and fused to negatively charged Kupffer cells via the HVJ envelope on their surfaces, reaching the cell nuclei directly without being subject to endosomal or lysosomal digestion [23, 24]. The high transfection efficiency of HVJ cationic liposomes in comparison with conventional cationic liposomes without HVJ seemed to be partly due to this difference in the mechanism of the incorporation of the ODN.

For in vivo gene transfer, the route of administration is one of the most important factors determining the efficiency. Peripheral intravenous injection [16–20, 22] and direct injection into the visceral peritoneum of the liver [15] have been reported using liposome vectors. When injected via the peripheral vein, the liposomes tend to form aggregates in vessels and rapidly accumulate in the lung [18], and thus it takes longer for the liposomes to be delivered to the liver (24 h to 7 days) [16, 18, 20, 22]. We administered the conventional cationic liposomes without HVJ via the portal vein instead of via peripheral veins to improve the transfection efficiency and shorten the time for the delivery of the liposomes. However, the efficiency was almost the same as that with intravenous injection. When injecting the conventional cationic liposomes without HVJ via the portal vein, the incubation time of 15 min was too short for the liposomes to be endocytosed or phagocytosed by Kupffer cells. Thus, the liposomes injected via the portal vein passed through the liver, and portal injection was no more effective than intravenous injection. In contrast, when using HVJ liposomes, the

fusion between liposomes and cells occurred very rapidly, as shown in our in vitro study, and the incubation time of 15 min was long enough for the ODNs to be incorporated into the Kupffer cells. In contrast when injected intravenously, HVJ liposome was delivered to Kupffer cells at a low efficiency and it may be because HVJ liposomes were accumulated in other organs than liver and fused to the cells in such organs rapidly. In fact, the intraportal injection of HVJ liposomes caused no accumulation of liposomes in the heart, lungs, spleen or kidneys, while the intravenous injection caused accumulation in lung, spleen and kidneys (data not shown). When the visceral peritoneum is directly injected, the liposomes are transfected only into hepatocytes close to the site of injection [15]. Our results demonstrated that the intraportal injection of HVJ liposomes had no adverse effects on the liver. In addition, this method was found to be specific and efficient for targeting Kupffer cells. Regarding the clinical application of this technique, the portal vein can easily be injected during surgery and percutaneous transhepatic portal vein puncture guided by ultrasonography can also be safely performed.

HVJ liposomes have several advantages over viral vectors for in vivo gene transfection. Although adenovirus vector appears to be an attractive vehicle because of its efficient transfection in vivo at the first injection, it induces antibody production, resulting in the failure of repetitive injections [6]. In contrast, Hirano et al. [25] showed that the antibody response to HVJ liposomes was weak and transient upon repetitive beta-galactosidase gene transfection into the liver with HVJ liposomes. HVJ liposomes can be used for the transfection of various sizes of DNA, that is, either plasmid expression vectors or oligonucleotides [26]. In this study, we demonstrated the effectiveness of HVJ liposomes for the transfection of both these sizes of DNAs into Kupffer cells: both FITC-labeled ODN and pCAG-lacZ were transfected into Kupffer cells with high efficiency. The ease with which oligonucleotides can be encapsulated in HVJ liposomes is also advantageous. Antisense and decoy oligonucleotides have recently been introduced as specific modulators of gene expression in vitro. The HVJ liposome method has been reported to prolong the half-life of antisense oligonucleotides in vitro and in vivo, resulting in the improvement of transfection efficiency [8, 24, 27]. Morishita et al. [8, 28] reported that a single intraluminal administration of cdc2 kinase antisense and E2F decoy oligonucleotides encapsulated in HVJ liposomes inhibited neointima formation after a balloon injury of the rat carotid artery for up to 8 weeks in vivo. Furthermore, antisense oligonucleotides against TGF-β and TNF-α have been reported to inhibit TGF-β production in CCl4-injured rat livers [29] and lipopolysaccharide-induced TNF-α release in alveolar epithelial cells [30], respectively. Thus, the intraportal administration of HVJ cationic liposomes may be a potent method for the treatment of fibrosis and inflammatory injury of the liver in vivo when combined with antisense or decoy technology.

In conclusion, we have developed a novel technique for in vivo gene transfer to Kupffer cells, and this technique may prove to be a useful tool for both experimental and clinical applications for the treatment of liver disorders.

Acknowledgments

We should gratefully appreciate Dr. Yasufumi Kaneda at Institute for Cellular and Molecular Biology, Osaka University Medical School, for his generous gift of HVJ and technical advice. This work was supported in part by a grant from the Scientific Research Fund of the Ministry of Education, Sport, and Culture, Government of Japan and a grant from the Research for the Future of Japan Society for the Promotion of Science.

References

1 Diehl AM, Rai R: Review: Regulation of liver regeneration by pro-inflammatory cytokines. J Gastroenterol Hepatol 1996;11:466–470.
2 Boulton RA, Alison MR, Golding M, Selden C, Hodgson HJ: Augmentation of the early phase of liver regeneration after 70% partial hepatectomy in rats following selective Kupffer cell depletion. J Hepatol 1989;29:271–280.
3 Suzuki S, Toledo-Pereyra LH, Rodriguez F, Lopez F: Role of Kupffer cells in neutrophil activation and infiltration following total hepatic ischemia and reperfusion. Circ Shock 1994;42:204–209.
4 Wang P, Ba ZF, Chaudry IH: Mechanism of hepatocellular dysfunction during early sepsis: Key role of increased gene expression and release of proinflammatory cytokines tumor necrosis factor and interleukin-6. Arch Surg 1997; 132:364–369.
5 Jooss K, Yang Y, Wilson JM: Cyclophosphamide diminishes inflammation and prolongs transgene expression following delivery of adenoviral vectors to mouse liver and lung. Hum Gene Ther 1996;7:1555–1566.
6 Yang Y, Li Q, Ertl HCJ, Wilson JM: Cellular and humoral immune response to viral antigens create barriers to lung-directed gene therapy with recombinant adenovirus. J Virol 1995; 69:2004–2015.
7 Jung Kang U: Genetic modification of cells with retrovirus vectors for grafting into the central nervous system: Gene Therapy and Neuroscience Applications; in Kaplitt MG, Loewy AD (eds): Viral Vectors. San Diego, Academic Press, 1995, pp 215–216.

8 Morishita R, Gibbons GH, Ellison KE, Nakajima M, Zhang L, Kaneda Y, Ogihara T, Dzau VJ: Single intraluminal delivery of antisense cdc2 kinase and proliferating-cell nuclear antigen oligonucleotides results in chronic inhibition of neointimal hyperplasia. Proc Natl Acad Sci USA 1993;90:8474–8478.
9 Sawa Y, Kadoba K, Suzuki K, Bai HZ, Kaneda Y, Shirakura R, Matsuda H: Efficient gene transfer method into the whole heart through the coronary artery with hemagglutinating virus of Japan liposome. J Thorac Cardiovasc Surg 1997;113:512–519.
10 Dzau VJ, Mann MJ, Morishita R, Kaneda Y: Fusigenic viral liposome for gene therapy in cardiovascular diseases. Proc Natl Acad Sci USA 1996;93:11421–11425.
11 Kato K, Yoneda Y, Okada Y, Kiyama H, Shiosaka S: Gene transfer and the expression of a foreign gene in vivo in post-mitotic neurons of the adult rat brain using the hemagglutinating virus of the Japan-liposome method. Brain Res Mol Brain Res 1994;25:359–363.
12 Tomita N, Higaki J, Morishita R, Kato K, Mikami H, Kaneda Y, Ogihara T: Direct in vivo gene introduction into rat kidney. Biochem Biol Res Com 1992;186:129–134.
13 Kaneda Y, Iwai K, Uchida T: Increased expression of DNA cointroduction with nuclear protein in adult rat liver. Science 1989;243:375–378.
14 Uehara T, Honda K, Hatano E, Terao R, Iimuro Y, Yamamoto N, Yamamoto M, Kaneda Y, Yamaoka Y: Gene transfer to the rat biliary tract with the HVJ-cationic liposome method. J Hepatol 1999;30:836–842.
15 Kato K, Nakanishi M, Kaneda Y, Uchida T, Okada Y: Expression of hepatitis B virus surface antigen in adult rat liver: Co-introduction of DNA and nuclear protein by a simplified liposome method. J Biol Chem 1991;266:3361–3364.
16 Alino SF, Bobadilla M, Garcia-Sanz M, Lejarreta M, Unda F, Hilario E: In vivo delivery of human α1-antitrypsin gene to mouse hepatocytes by liposomes. Biochem Biophys Res Commun 1993;192:174–181.
17 Bugelski PJ, Gennaro DE, Poste G, Hoffstein ST: A new cytochemical method for ultrastructural detection of liposomes in tissues in vivo. J Histochem Cytochem 1989;37:843–851.
18 Litzinger DC, Brown JM, Wala I, Kaufman SA, Van GY, Farrell CL, Collins D: Fate of cationic liposomes and their complex with oligonucleotide in vivo. Biochim Biophys Acta 1996;1281:139–149.
19 Kawakami S, Wong J, Sato A, Hattori Y, Yamashita F, Hashida M: Biodistribution characteristics of mannosylated, fucosylated, and galactosylated liposomes in mice. Biochim Biophys Acta 2000;1524:258–265.
20 Reinders ME, Wagensveld BA, Gulik TM, Corssmit NPM, Frederiks WM, Chamuleau RA, van Rooijen N, Obertop H: No attenuation of ischemic and reperfusion injury in Kupffer cell-depleted, cold-preserved rat liver. Transplantation 1997;63:449–454.
21 MacSween RNM, Scothorne RJ: Developmental anatomy and normal structure; in MacSween RNM, Anthony PP, Scheuer PJ, Burt AD, Portmann BC (eds): Pathology of the Liver, ed 3. New York, Churchill Livingstone, 1994, p 29.
22 Chow DD, Essien HE, Milind MP, Hwang KJ: Targeting small liposomes to hepatic parenchymal cells by dose effect. J Pharmacol Exp Ther 1989;248:506–513.
23 Okada Y, Koseki I, Hashimoto T, Kanno Y, Matsui Y: Modification of cell membranes with viral envelops during fusion of cells with HVJ (Sendai virus). Exp Cell Res 1975;93:368–378.
24 Morishita R, Gibbons GH, Kaneda Y, Ogihara T, Dzau VJ: Pharmacokinetics of antisense oligodeoxyribonucleotides (cyclin B1 and CDC2 kinase) in the vessel wall in vivo: Enhanced therapeutic utility for restenosis by HVJ-liposome delivery. Gene 1994;149:13–19.
25 Hirano T, Fujimoto J, Ueki T, Yamamoto H, Iwasaki T, Morisita R, Sawa Y, Kaneda Y, Takahashi H, Okamoto E: Persistent gene expression in rat liver in vivo by repetitive transfections using HVJ-liposome. Gene Ther 1998;5:459–464.
26 Ellison KE, Bishopric NH, Webster KA, Morishita R, Gibbons GH, Kaneda Y, Sato B, Dzau VJ: Fusigenic liposome-mediated DNA transfer into cardiac myocytes. J Mol Cell Cardiol 1996;28:1385–1399.
27 Tomita N, Morishita R, Higaki J, Aoki M, Nakamura Y, Mikami H, Fukamizu A, Murakami K, Kaneda Y, Ogihara T: Transient decrease in high blood pressure by in vivo transfer of antisense oligodeoxynucleotides against rat angiotensinogen. Hypertension 1995;26:131–136.
28 Morishita R, Gibbons GH, Horiuchi M, Ellison KE, Nakama M, Zhang L, Kaneda Y, Ogihara T, Dzau VJ: A gene therapy strategy using a transcription factor decoy of the E2 binding site inhibits smooth muscle proliferation in vivo. Proc Natl Acad Sci USA 1995;92:5855–5859.
29 Armendariz-Borunda J, LeGros L Jr, Campollo O, Panduro A, Rincon AR: Antisense S-oligodeoxynucleotides down-regulate TGF-beta production by Kupffer cells from CCl4-injured rat livers. Biochim Biophys Acta 1997;1353:241–252.
30 Xavier AM, Isowa N, Cai L, Dziak E, Opas M, McRitchie DI, Slutsky AS, Keshavjee SH, Liu M: Tumor necrosis factor-alpha mediates lipopolysaccharide-induced macrophage inflammatory protein-2 release from alveolar epithelial cells. Autoregulation in host defense. Am J Respir Cell Mol Biol 1999;21:510–520.

Am J Physiol Gastrointest Liver Physiol 282: G962–G971, 2002.
First published January 30, 2002; 10.1152/ajpgi.00466.2001.

Effect of heat shock preconditioning on NF-κB/I-κB pathway during I/R injury of the rat liver

HIROSHI UCHINAMI, YUZO YAMAMOTO, MAKOTO KUME, KEI YONEZAWA, YASUHIDE ISHIKAWA, KOJIRO TAURA, AKIO NAKAJIMA, KOICHIRO HATA, AND YOSHIO YAMAOKA
Department of Gastroenterological Surgery, Graduate School of Medicine, Kyoto University, Kyoto 606–8507, Japan

Received 1 November 2001; accepted in final form 29 January 2002

Uchinami, Hiroshi, Yuzo Yamamoto, Makoto Kume, Kei Yonezawa, Yasuhide Ishikawa, Kojiro Taura, Akio Nakajima, Koichiro Hata, and Yoshio Yamaoka. Effect of heat shock preconditioning on NF-κB/I-κB pathway during I/R injury of the rat liver. *Am J Physiol Gastrointest Liver Physiol* 282: G962–G971, 2002. First published January 30, 2002; 10.1152/ajpgi.00466.2001.—Hepatic ischemia-reperfusion (I/R) injury continues to be a fatal complication after liver surgery. Heat shock (HS) preconditioning is an effective strategy for protecting the liver from I/R injury, but its exact mechanism is still unclear. Because the activation of nuclear factor-κB (NF-κB) is an important event in the hepatic I/R-induced inflammatory response, the effect of HS preconditioning on the pathway for NF-κB activation was investigated. In the control group, NF-κB was activated 60 min after reperfusion, but this activation was suppressed in the HS group. Messenger RNA expressions of proinflammatory mediators during reperfusion were also reduced with HS preconditioning. Concomitant with NF-κB activation, NF-κB inhibitor I-κB proteins were degraded in the control group, but this degradation was suppressed in the HS group. This study shows that HS preconditioning protected the liver from I/R injury by suppressing the activation of NF-κB and the subsequent expression of proinflammatory mediators through the stabilization of I-κB proteins.

hepatic ischemia-reperfusion; nuclear factor-κB proinflammatory mediators

AN ORGANISM HAS ENDOGENOUS ability to respond to environmental stresses for survival (37, 39). This highly conserved response is called the "stress response" and is associated with the expression of a wide spectrum of proteins related to organic defense mechanisms. For example, the induction of oxygen-free radical scavenging enzymes (12, 26) and several members of the heat shock protein (HSP) family (5, 35, 52), particularly HSP-72, have been noted. HSP-72 functions as a molecular chaperone (23, 25) and contributes to the folding, assembling, and stabilization of intracellular proteins. It is believed that HSP-72 enables an organism to survive noxious stresses (10, 38). We have previously reported that heat shock (HS) preconditioning reduces liver damage caused by ischemia-reperfusion (I/R) injury resulting in a remarkable increase in survival rate (31, 44, 59, 60). We have also demonstrated a correlation between HS preconditioning-induced expression levels of HSP-72 in the liver and resulting tolerance against hepatic I/R injury. I/R injury facilitates the depletion of ATP, the deterioration of intracellular Ca^{2+} homeostasis (4, 21), the activation of cytotoxic enzymes (proteases, phospholipases, arachidonic acid, etc.) (20), and the generation of reactive oxygen species (ROS) (17). However, little is known about the mechanism with which HS preconditioning or HSP-72 provides protection against hepatic I/R injury.

It has recently been shown that several signaling pathways are activated in response to hepatic I/R, and the activated transcription factors induce a variety of cellular gene expressions. For example, nuclear factor-κB (NF-κB) is a ubiquitous, inducible transcription factor that regulates the expression of numerous cellular genes, particularly those involved in the inflammatory response (2). Recently, its activation during hepatic I/R has been well documented (64–66). NF-κB is retained in cytoplasm by its inhibitor I-κB proteins. In response to a variety of stimuli, cytoplasmic NF-κB/I-κB complex is disassociated, and free NF-κB is then allowed to migrate into the nucleus where it can bind to cognate DNA binding sites (2). We hypothesized that the protective action of HS preconditioning on I/R injury might be mediated by, at least in part, the suppression of NF-κB activation. In this study, we evaluated the effect of HS preconditioning on the NF-κB/I-κB pathway using a hepatic I/R model in rats. We also sought to determine the role of HS preconditioning on the expression of proinflammatory mediators during I/R of the liver.

MATERIALS AND METHODS

Experimental model and animals. We have previously reported that HS preconditioning protects the liver from I/R injury by the use of a rat model of 30-min hepatic ischemia with 15-min HS preconditioning 48 h before ischemia. In this

Address for reprint requests and other correspondence: Y. Yamamoto, Dept. of Gastroenterological Surgery, Graduate School of Medicine, Kyoto University, 54 Kawahara-cho, Shogoin, Sakyo-ku, Kyoto 606–8507, Japan (E-mail: mai@kuhp.kyoto-u.ac.jp).

The costs of publication of this article were defrayed in part by the payment of page charges. The article must therefore be hereby marked "*advertisement*" in accordance with 18 U.S.C. Section 1734 solely to indicate this fact.

model, protective effects were clearly demonstrated with serum liver-related enzyme levels, recovery of hepatic ATP and energy charge levels, and survival rate (31, 44, 59). Therefore, the same animal model was employed in the present study.

Experiments were performed with male Wistar rats (obtained from Shizuoka Laboratory Animal Center, Shizuoka, Japan) weighing between 280 and 320 g. They were housed in a climatized room with a 12:12-h light-dark cycle and had free access to water and food. They received humane care in compliance with the Animal Protection Guidelines of Kyoto University.

Preconditioning. Rats were divided into either an HS group (*group HS*) or control group (*group C*). To monitor their rectal temperature, all rats were anesthetized with pentobarbital sodium (40 mg/kg ip) and fitted with a thermocouple probe inserted in the rectum 2–3 cm beyond the anal sphincter. Because rectal temperature during HS treatment shows good parallelism with the directly measured liver temperature, as reported elsewhere (31), we monitored rectal temperature in place of liver temperature in this study. Rats in *group HS* were bathed in 42.5°C water until their rectal temperature reached 42°C and were then moved to 41.5°C water to maintain their temperatures at 42°C for 15 min. In *group C*, rats were bathed in a 37°C water bath for 35 min to proximate the total duration of preconditioning in *group HS*, which was 35–40 min. Rats were allowed to recover from anesthesia and were returned to their cages.

I/R. Rats from both pretreatment groups recovered for 48 h and were anesthetized again. A midline laparotomy was performed, and total hepatic ischemia was induced by clamping the hepatoduodenal ligament for 30 min using an atraumatic microvascular clip (Pringle's maneuver). Reperfusion was accomplished by removing the clip. At several indicated time points, rats were killed by exsanguination. Their liver tissue was taken for analysis and stored in liquid nitrogen until use.

Preparation of whole cell, nuclear, and cytoplasmic extracts. Liver tissue was rinsed with PBS and then homogenized on ice in 3 ml of buffer containing (in mM) 50 Tris·HCl (pH 7.5), 150 NaCl, 1 1,4-dithiothreitol (DTT), 1 phenylmethylsulfonyl fluoride (PMSF), protease inhibitor cocktail (Roche, Mannheim, Germany), 50 NaF, and 0.1 Na_3VO_4, with 0.05% Triton X-100 using a Potter homogenizer. The homogenates were incubated for 15 min on ice and centrifuged at 15,000 *g* for 20 min. The supernatants were stored at −80°C as whole cell extracts. For the isolation of nuclear and cytoplasmic protein extracts, a procedure modified from the method of Zwacka et al. (65) was used. Briefly, liver tissue was rinsed with ice-cold PBS and homogenized on ice in 6 ml of ice-cold *buffer A* [in mM: 10 mM HEPES (pH 7.9), 1.5 $MgCl_2$, 10 NaCl, 1 DTT, 1 PMSF, 50 NaF, and 0.1 Na_3VO_4, with protease inhibitor cocktail] using a Potter homogenizer. After a 10-min incubation on ice, the homogenate was transferred to a polypropylene centrifuge tube and centrifuged at 850 *g* for 10 min at 4°C. The supernatants were stored as cytoplasmic extracts at −80°C. The pellet was suspended in an ice-cold *buffer B* (0.1% Triton X-100 in *buffer A*), incubated on ice for 10 min, and then centrifuged as above. The crude nuclear pellet was resuspended in *buffer C* (*buffer A* with 1.7 M sucrose) and overlaid on 1 ml of cushion buffer (*buffer A* with 2.2 M sucrose) followed by centrifugation at 75,000 *g* for 2 h at 4°C. The supernatant was removed, and the purified nuclear pellet was resuspended in 250 μl of Dignam C buffer [20 mM HEPES (pH 7.9), 1.5 mM $MgCl_2$, 0.42 M NaCl, 25% glycerol, 0.2 mM EDTA, 1 mM PMSF, 1 mM DTT, and protease inhibitor cocktail]. The suspension was incubated for 30 min at 4°C with frequent vortexing. After the supernatants were centrifuged at 15,000 *g* for 15 min at 4°C, they were transferred to new tubes in aliquotes to freeze in liquid nitrogen and stored at −80°C until use.

The protein concentration of each extract was determined by bicinchoninic acid (BCA) protein assay reagent using bovine serum albumin as a reference standard (Pierce, Rockford, IL).

Electrophoretic mobility shift assay. A modified procedure based on the method of Diaz-Guerra et al. (16) was used. The NF-κB binding sequence, derived from the murine inducible nitric oxide synthase (iNOS) promoter and also containing a functional NF-κB element (5′-CCAACTGGGGACT-CTCCC-TTTGGGAACA-3′) was used as a probe. Double-stranded oligonucleotide was end-labeled with [γ-^{32}P]ATP (3,000 Ci/mmol at 10 mCi/ml; Amersham Pharmacia Biotechnology, Tokyo, Japan) using T4 polynucleotide kinase (Nippon gene, Toyama, Japan) and purified in G-50 sephadex columns (Roche). Nuclear extracts (10 μg) were incubated with electrophoretic mobility shift assay (EMSA) buffer [in mM: 10 Tris·HCl (pH 7.5), 50 NaCl, 1 MgCl2, 1 EDTA, and 1 DTT, with 4% glycerol (vol/vol) and 1μg poly(dI-dC)] in a final volume of 14 μl for 15 min at 4°C, and then incubated with 1μl of radiolabeled oligonucleotide (35 fmol/μl) for 20 min at room temperature. DNA-protein complexes were analyzed on a 5% native polyacrylamide gel run in 0.25 × Tris borate/EDTA buffer for 90 min at 150 mV. In a competition assay, a 100-fold molar excess of nonradioactive NF-κB or activator protein-1 (AP-1) oligonucleotides was added to the binding reaction for 1 h before the addition of radiolabeled probes. In a supershift analysis, the binding reaction, containing 1μg of anti-p50 or -p65 antibodies (Santa Cruz Biotechnology, Santa Cruz, CA), was incubated for 1 h on ice before adding radioactive probes. The dried gel on Whatman No. 3 MM paper (Whatman, Maidstone, UK) was exposed to an imaging plate and visualized on Fuji BAS 2000 apparatus (Fuji, Tokyo, Japan).

Semiquantitative RT-PCR. From liver tissue, total RNA was extracted using TRIzol reagent (GIBCO-BRL, Life Technologies, Rockville, MD) and was treated with deoxyribonuclease (RT grade; Nippon gene) for 15 min at 37°C to avoid DNA contamination during the PCR. RNA (5 mg) was reverse transcribed using a first-strand cDNA kit (Amersham Pharmacia Biotechnology, Buckinghamshire, UK) in a 15-μl reaction mixture according to the manufacturer's protocol. Because the performance of PCR was exclusively higher for β-actin cDNA than other cDNAs, the RT products were amplified in a two-step PCR (32) using *Taq* DNA polymerase (GIBCO-BRL) and specific cDNA primers for iNOS, tumor necrosis factor-α (TNF-α), and macrophage inflammatory protein-2 (MIP-2). β-Actin cDNA was coamplified as an internal standard. Primers used in the PCR were as follows: TNF-α 5′ primer (5′-CACGCTCTTCTGTCTACTGA-3′) and TNF-α 3′ primer (5′-GGACTCCGTGATGTCTAAGT-3′) to give a 541-bp product; β-actin 5′ primer (5′-CTACAAT-GAGCTGCGTGTGG-3′) and β-actin 3′ primer (5′-CGCGTA-ACCCCATAGA-TGG-3′) to give a 241-bp product; and diluted iNOS and MIP-2 primer pairs (Biosource, Camarillo, CA) to give 563- and 219-bp products, respectively. Each PCR cycle consisted of a heat-denaturation step at 94°C for 30 s, annealing of primers at 60°C for 45 s, and polymerization at 72°C for 45 s. The PCRs for TNF-α, MIP-2, and iNOS were first initiated for 8, 8, and 10 cycles, respectively, using only their specific primers. After the first-step PCR, primers for β-actin were added to the reaction mixture and an additional 20 cycles of amplification were carried out. These PCR cycle numbers were determined by a kinetic study (22–34 cycles)

for each set of primers to ensure that all PCR products remain proportional to initial gene expression templates. The PCR products were run on 2.5% agarose gel, stained with ethidium bromide, and then visualized by ultraviolet illumination. Signal intensities were evaluated using Bio-Rad's image-analysis systems (Bio-Rad, Hercules, CA). The levels of iNOS, TNF-α, and MIP-2 mRNA were normalized to the level of β-actin mRNA. Results were expressed in arbitrary units.

Western blot analysis. Western blotting was performed according to a method described elsewhere (31). Nuclear, cytoplasmic or whole cell, extract was boiled for 5 min in equal volumes of 2× sample buffer [250 mM Tris·HCl (pH 6.8), 4% SDS, 10% glycerol, 2% β-mercaptoethanol, and 0.003% blomophenol blue] at 95°C. Protein samples (20 μg) were separated on denaturing 10% SDS-polyacrylamide gels and transferred to a polyvinylidene fluoride membrane (Millipore, Tokyo, Japan) using a semidry transfer system (Bio-Rad). The gels were stained with Coomassie to ensure that equal amounts of loading proteins were used. The membranes were blocked overnight at 4°C with a blocking buffer (5% nonfat dry milk in PBS with 0.1% Tween 20). Membranes were washed three times for 5 min in PBS containing 0.05% Tween 20 (TPBS) and then incubated for 2 h at room temperature with polyclonal rabbit anti-p65 antibody (1:2,000 dilution; Santa Cruz), anti-I-κBα antibody (1:2,500 dilution; Santa Cruz), polyclonal rabbit anti-I-κBβ antibody (1:2,000 dilution; Santa Cruz), monoclonal mouse anti-HSP-72 antibody (1:3,000 dilution; StressGen, Victoria, Canada), monoclonal mouse anti-HSP-60 antibody (1:2,000 dilution; StessGen), and monoclonal mouse anti-HSP-90 antibody (1:2,000 dilution; StressGen) in blocking buffers. Membranes were washed three times in TPBS for 10 min and incubated for 1 h at room temperature with an appropriate secondary antibody (anti-rabbit or anti-mouse IgG conjugated with horseradish peroxidase (1:1,500 dilution; Santa Cruz) in TPBS. After the membranes were washed four times in TPBS for 15 min, they were developed with the enhanced chemiluminescence system (Amersham Pharmacia Biotechnology) according to the manufacturer's protocol and then exposed to films. Protein levels were quantified by scanning densitometry using image-analysis systems (Bio-Rad). Expression levels of I-κBs were evaluated by their relative integrated intensity vs. a normal liver and presented as a percentage of the standard.

Kinase assay. For measuring I-κB kinase (IKK) activity, kinase assay was performed, with some modifications, using the method of Schwabe et al. (49). Extracts were prepared by incubating liver tissue in lysis buffers [20 mM Tris·HCl (pH 7.5), 200 mM NaCl, 10% glycerol, 0.5% Nonidet P-40 (NP-40), 50 mM NaF, 0.1 mM Na_3VO_4, 1 mM DTT, protease inhibitor cocktail, 1 mM PMSF, and 20 mM β-glycerophosphate]. Protein concentrations were determined using the BCA method. Three milligrams of protein were precleared in a 900-μl pull-down buffer [20 mM Tris·HCl (pH 7.5), 200 mM NaCl, 10% glycerol, 0.05% NP-40, and 2 mM EDTA] containing protease and phosphatase inhibitor for 30 min at 4°C on a rocking platform by adding 30 μl of protein A-agarose (Roche). After centrifugation, 2 μg of anti-NF-κB essential modulator (NEMO) antibody (Santa Cruz) was added to the supernatant and incubated overnight with continuous rocking at 4°C. Then, 30 μl of protein A-agarose were added to the samples, and they were incubated for another 3 h at 4°C. Precipitates were washed twice in pull-down buffers and twice in kinase buffers [in mM: 20 HEPES (pH 7.5), 20 MgCl2, 1 EDTA, 2 DTT, 20 β-glycerophosphate, 1 NaF, and 0.1 Na_3VO_4]. The kinase reaction was performed for 30 min at 30°C in a 30-μl kinase buffer containing 3μCi of [γ-^{32}P]ATP, 20μM ATP, and 1 μg of glutathione S-transferase-I-κBα substrate (Santa Cruz). The reactions were terminated by addition a 2× sample buffer, and the reaction mixtures were resolved on 10% SDS-acrylamide gels. After electrophoresis, the gels were dried and exposed at −80°C to Kodak X-ray films.

Statistical analysis. The significance of differences was determined by ANOVA. A P value < 0.05 was considered to be significant.

RESULTS

HS preconditioning induced production of HSP-72. To examine the stress response after HS preconditioning, we investigated protein expressions of three major HSPs (HSP-60, -72, and -90) in the liver tissue 48 h after preconditioning. As shown in Fig. 1, HSP-60 and -90 were constitutively expressed in the liver tissue. Compared with normal rat liver tissue, the expression of HSP-60 was not significantly enhanced in either *group C* or HS. The expression of HSP-90 was slightly increased in *group HS*. In livers of no-treatment and *group C* rats, HSP-72 was hardly detectable but was induced strongly in the liver of *group HS*.

HS preconditioning inhibited NF-κB activation during I/R. To assess the effect of HS preconditioning on the DNA binding activity of NF-κB during hepatic I/R, EMSA was performed on nuclear extracts obtained from livers undergoing a 30-min ischemia and a 60-min reperfusion. Two NF-κB/DNA complexes, presented as upper- and lower-band complexes appeared in *group C*. In contrast, only a weak lower-band complex was detected in *group HS* (Fig. 2*A*).

Specificity of these complexes for NF-κB was examined. Unlabeled NF-κB oligonuleotide of 100-fold excess inhibited formation of both NF-κB/DNA complexes (Fig. 2*B*, *lane 4*). However, the same excess of unrelated oligonucleotide (AP-1) had no effect (Fig. 2*B*, *lane 5*). These data indicated that both complexes were specific to NF-κB. Supershift assay using p50 antibody shifted both bands (Fig. 2*B*, *lane 2*), whereas only the upper-band complex was supershifted using p65 antibody (Fig. 2*B*, *lane 3*). These results illustrate that the complexes detected by EMSA corresponded to p50/p65 heterodimer and p50/p50 homodimer for the upper and lower bands, respectively.

Figure 2*C* illustrates the DNA binding activity of NF-κB during the time course of hepatic I/R. NF-κB binding activity increased by 60 min after reperfusion and remained elevated after 120 min in *group C*. But in *group HS*, this activation was not observed at any time. This suggests that HS preconditioning inhibits the increase in DNA binding activity of NF-κB during I/R in the liver.

To investigate whether this inhibitory effect on the DNA binding activity of NF-κB was associated with its translocation into the nucleus, Western blot analysis was performed with nuclear extract using p65 antibody (Fig. 2*D*). With results similar to the results of EMSA, the presence of a p65 subunit was demonstrated at 60 and 120 min after reperfusion in the nuclear extracts

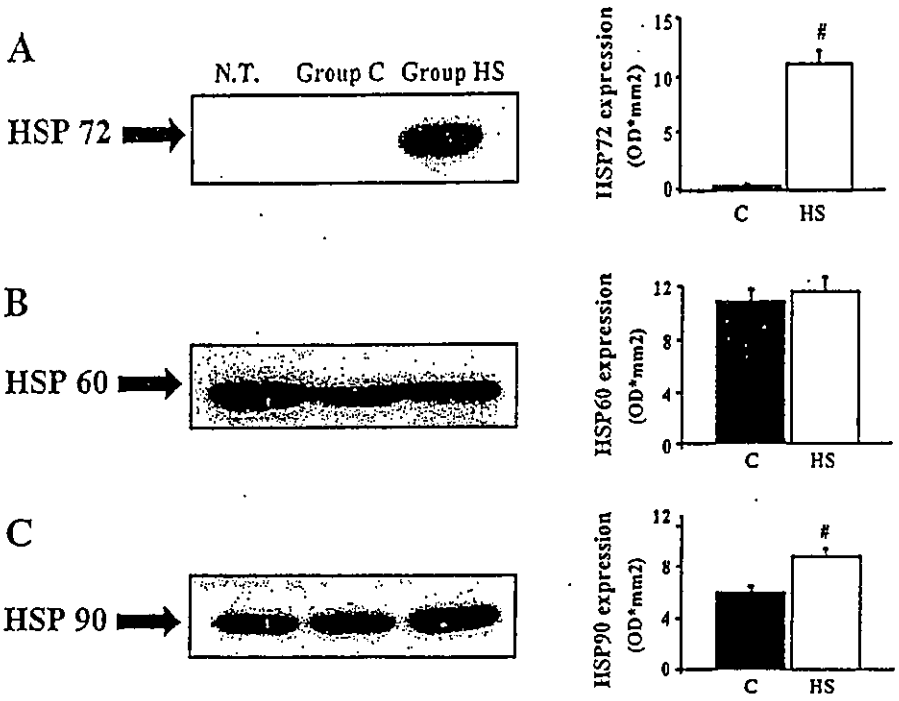

Fig. 1. The expression of heat shock (HS) proteins (HSPs) in livers was analyzed using Western blotting (*left*) and was evaluated by band intensity on the same film (*right*). *A*: HSP-72 was not expressed in the livers of control (C) group (*group C*; 48 h after 37°C treatment) and no-treatment livers (NT). However, it was strongly expressed in an HS group (*group HS*; 48 h after 42°C treatment). *B*: HSP-60 was constitutively expressed, and there was no difference in its expression level between the groups. *C*: HSP-90 was expressed in both groups. The amount of HSP-90 was slightly increased in *group HS*. All data were expressed as the means ± SE ($n = 5$ in each group). #$P < 0.01$ vs. *group C*. OD, optical density.

in *group C*, but it was not detected in *group HS*. To investigate whether HS preconditioning suppresses NF-κB activation by decreasing the cytoplasmic p65 expression, we also measured p65 protein levels at 48 h after HS. But p65 level in the cytoplasmic fraction did not change after HS preconditioning. This suggests that HS preconditioning-mediated inhibition of DNA binding activity of NF-κB was not due to the decrease in the amount of p65 but to the inhibition of some signaling pathway upstream of the translocation of NF-κB into the nucleus.

HS preconditioning suppressed expression of iNOS, TNF-α, and MIP-2 mRNA at 120 min after reperfusion. Because activation of NF-κB is required for the transcription of proinflammatory mediators, we examined whether production of mRNA for these mediators was suppressed after hepatic I/R by HS preconditioning. mRNA levels of iNOS, TNF-α, and MIP-2 were assessed by RT-PCR using RNA extracts from liver tissue before ischemia and at 120 min after reperfusion. Before ischemia, the mRNA expression of these mediators was not detected in either group. At 120 min after reperfusion, levels of these mRNA expressions were increased in *group C*, but the increase was significantly abrogated in *group HS* (Fig. 3). These data showed that HS preconditioning inhibited the mRNA expression of NF-κB responsible genes.

HS preconditioning increased I-κB family proteins and prevented their degradation during I/R. Activation of NF-κB is largely dependent on the degradation of I-κB family proteins. To delineate the temporal profile of I-κBs during I/R, protein levels of I-κBα and I-κBβ were assessed by Western blot analysis using cytoplasmic extracts (Fig. 4). In the cytoplasm of *group C*, expression levels of both I-κBs began to decrease at the end of ischemia and showed minimal levels between 30 and 60 min after reperfusion. These levels increased gradually toward 120 min after reperfusion. On the other hand, preischemic levels of I-κBα and I-κBβ were significantly higher in *group HS* than in *group C*. In addition, HS preconditioning prevented I/R-induced decrease in I-κB family protein. It was therefore demonstrated that HS preconditioning induced an increase in cytoplasmic I-κB proteins and prevented their degradation during hepatic I/R.

IKK complex was not activated during hepatic I/R. A number of studies has demonstrated that the degradation of I-κB requires serine phosphorylation mediated by IKK. IKK is a complex composed of three subunits: IKKα, IKKβ, and NEMO (36, 61). Because hepatic I/R caused the degradation of I-κB proteins, we hypothesized that the activation of the IKK complex during I/R and the suppression of this activation by HS preconditioning resulted in maintaining the quantity of I-κB protein. To investigate this possibility, activities of IKK complex during hepatic I/R were examined using an immunocomplex kinase assay (Fig. 5). However, no increase in IKK activity was detected during the I/R period in *group C* or in *group HS*.

DISCUSSION

In the liver, I/R induces proinflammatory mediators such as TNF-α, adhesion molecules, chemokines, and iNOS. These locally overexpressed hepatic proinflammatory mediators play a critical role in the progression of hepatic I/R damage (6–8, 18, 29, 34). Expression of these mediators initiates the activation of the inflammatory cascade, leading to hepatic neutrophil recruitment, microcirculatory disturbance, and hepatic dys-

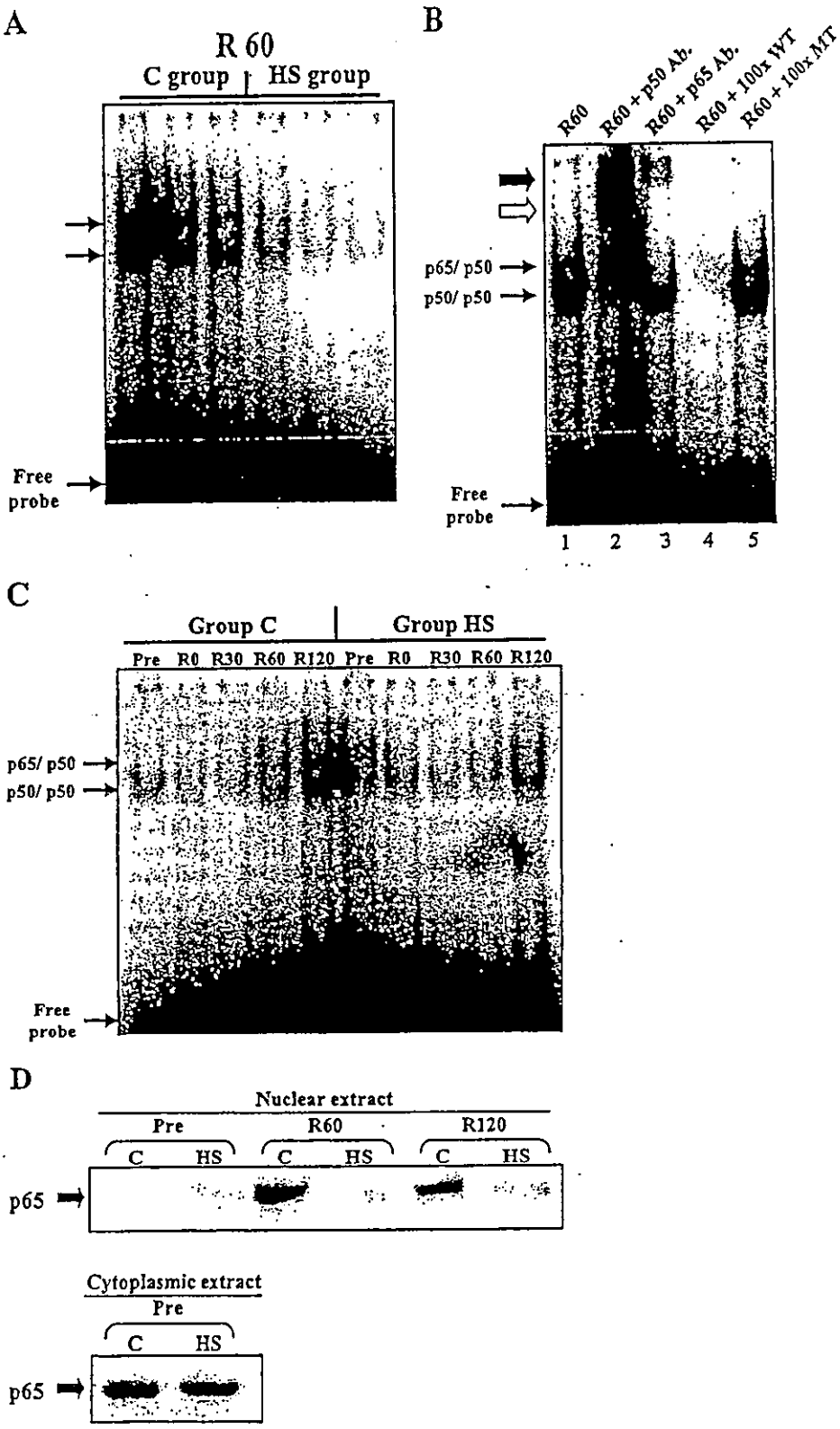

Fig. 2. Nuclear factor-κB (NF-κB) activation during hepatic ischemia-reperfusion. *A*: the electrophoretic mobility shift assay (EMSA) was performed to determine the NF-κB DNA binding activity in the nuclear extracts from livers obtained 60 min after reperfusion. NF-κB activation was clearly demonstrated 60 min after reperfusion in *group C*, but activation was not observed in *group HS*. EMSA assay was triplicated in both groups using 3 independent samples. *B*: specificity of the NF-κB/DNA complex was confirmed by a supershift assay. *Lane 1* shows EMSA 60 min after reperfusion in *group C*. *Lanes 2* and *3* show the supershift assay using antibodies (Ab) of p50 (*lane 2*) and p65 (*lane 3*). *Lanes 5* and *6* show the competition assay with 100× excess molar of unlabeled NF-κB oligonucleotide (*lane 4*) and activator protein-1 (AP-1) oligonucleotide (*lane 5*). The open arrow indicates a supershift band of p50, and the closed arrow indicates a supershift band of p65. *C*: a time course of NF-κB activation during hepatic ischemia-reperfusion. Nuclear extracts prepared from liver samples obtained at the preischemic phase (48 h after preconditioning) and at 0, 30, 60, and 120 min postreperfusion were subjected to EMSA. *D*: the expression level of NF-κB subunit, p65, in the nucleus. Nuclear extracts from livers obtained at the preischemic phase and at 60 and 120 min postreperfusion were subjected to Western blotting. *D*: the expression of p65 in cytoplasmic extract from the liver obtained at the preischemic phase was also evaluated to confirm that p65 was not affected by HS preconditioning. Pre, before ischemia; R0, just after ischemia; R30, 30 min after reperfusion; R60, 60 min after reperfusion; R120, 120 min after reperfusion.WT, wild-type oligonucleotide; MT, mutant oligonucleotide.

function. At the transcriptional level, each of these mediators is commonly controlled, at least in part, by NF-κB (9, 51, 53, 58). Accordingly, many investigators have studied the role of NF-κB activation during I/R in various organs and have suggested that the activation of NF-κB seems to be an early step in the pathogenesis of I/R injury. The beneficial effect of NF-κB inhibition on attenuating I/R damage is supported by the studies.

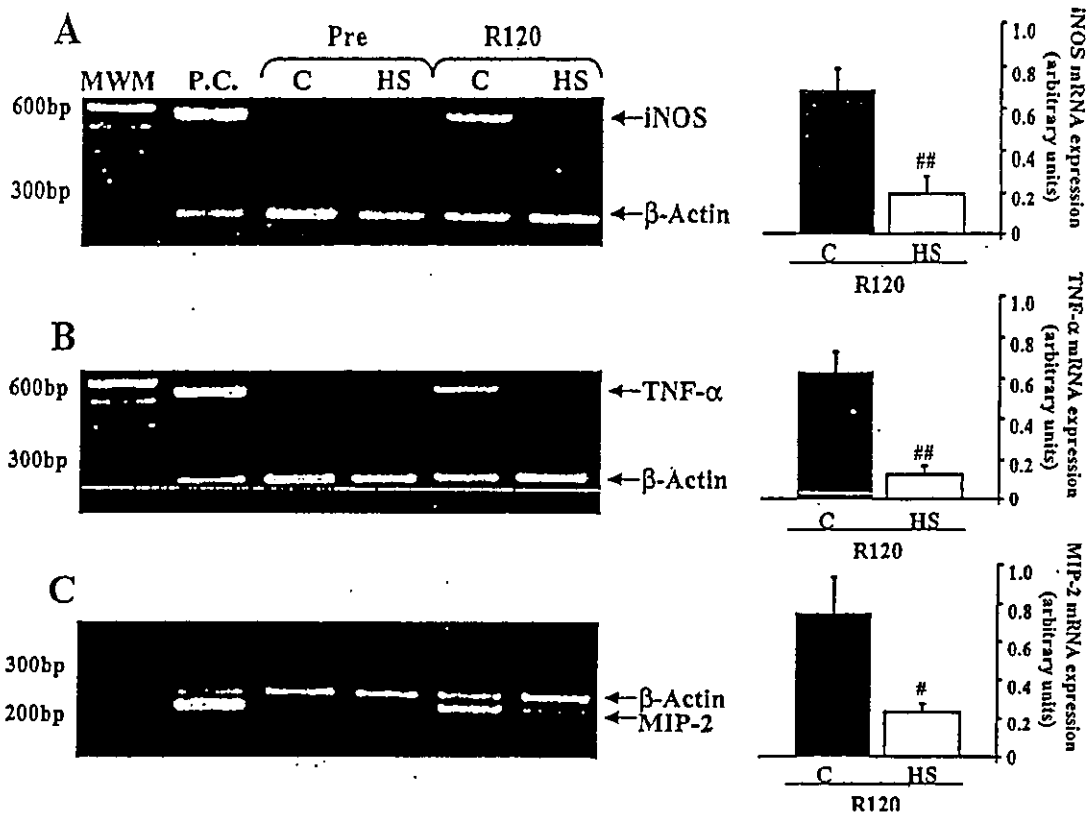

Fig. 3. Messenger RNA expression of inducible nitric oxide synthase (iNOS; *A*), tumor necrosis factor-α (TNF-α; *B*), and macrophage inflammatory protein-2 (MIP-2; *C*) in the liver. Total RNA from livers obtained at the preischemic phase and 120 min after reperfusion was subjected to RT-PCR using iNOS, TNF-α, and MIP-2 specific primers. β-actin was coamplified as a reference for quantitation of mRNA. A 2-step PCR method was employed for amplifying RT products. The PCRs for TNF-α, MIP-2, and iNOS were first initiated for 8, 8, and 10 cycles, respectively, using only their specific primers. After the first-step PCR, primers for β-actin were added to reaction mixture and an additional 20 cycles of amplification were carried out. PCR products were stained by ethidium bromide and photographed (*left*). RT-PCR products from the liver obtained 120 min after reperfusion were digitized using an image-analysis system, and the band intensity was normalized to β-actin (*right*). Results were expressed as the means ± SE ($n = 5$ in each group). #$P < 0.05$ and ##$P < 0.01$ vs. *group C*. PC, positive control [mRNA of the liver harvested 2 h after lipopolysaccharide injection (2 mg/kg)]; MWM, molecular weight marker.

One demonstrated that cerebral I/R injury was attenuated in p50 knockout mice (47), and a second showed that in vivo transfection of NF-κB decoy oligodeoxynucleotides could prevent myocardial infarction (40). A third study tested several therapeutic interventions for hepatic I/R injury (e.g., redox gene therapy, administration of interleukin-10 or atrial natriuretic peptide) that resulted in the inhibition of NF-κB activation (22, 41, 64, 66), and another study illustrated how the inhibition of NF-κB activation by I-κB superrepressor decreased cell death from oxidative stress in a hepatocyte cell line (30).

We have previously reported that HS preconditioning protects the liver from I/R injury in rats (31, 44, 59, 60), but the mechanism of that protection remains unclear. In the present study, we demonstrated that induction of the stress response with HS preconditioning increases HSP-72 levels and suppresses I/R-induced NF-κB activation in the liver. These results are consistent with other in vivo and in vitro experiments in which the stress response was able to suppress NF-κB activation (14, 15, 19, 45, 54, 55). We confirmed that at 120 min after reperfusion, mRNA levels of NF-κB target genes (TNF-α, MIP-2, and iNOS) in the liver were also reduced by HS preconditioning. Although we assessed the expression of these mediators only at an mRNA level, a recent study demonstrated that HS preconditioning suppressed elevation of plasma concentration of TNF-α during I/R (62). These findings suggest that modulation of NF-κB activation during hepatic I/R by HS preconditioning may be one of the molecular mechanisms responsible for its hepatoprotective properties.

The major pathway for NF-κB activation depends on activation of the IKK complex, which leads to the phosphorylation of serine residue of I-κB and the degradation of I-κB via the ubiquitin-proteasome system (36, 61). Under specific circumstances, other systems for NF-κB activation have also been implicated. According to Zwacka et al. (65), during hepatic I/R, NF-κB activation was initiated not by serine phosphorylation, but by tyrosine phosphorylation of I-κB and was not

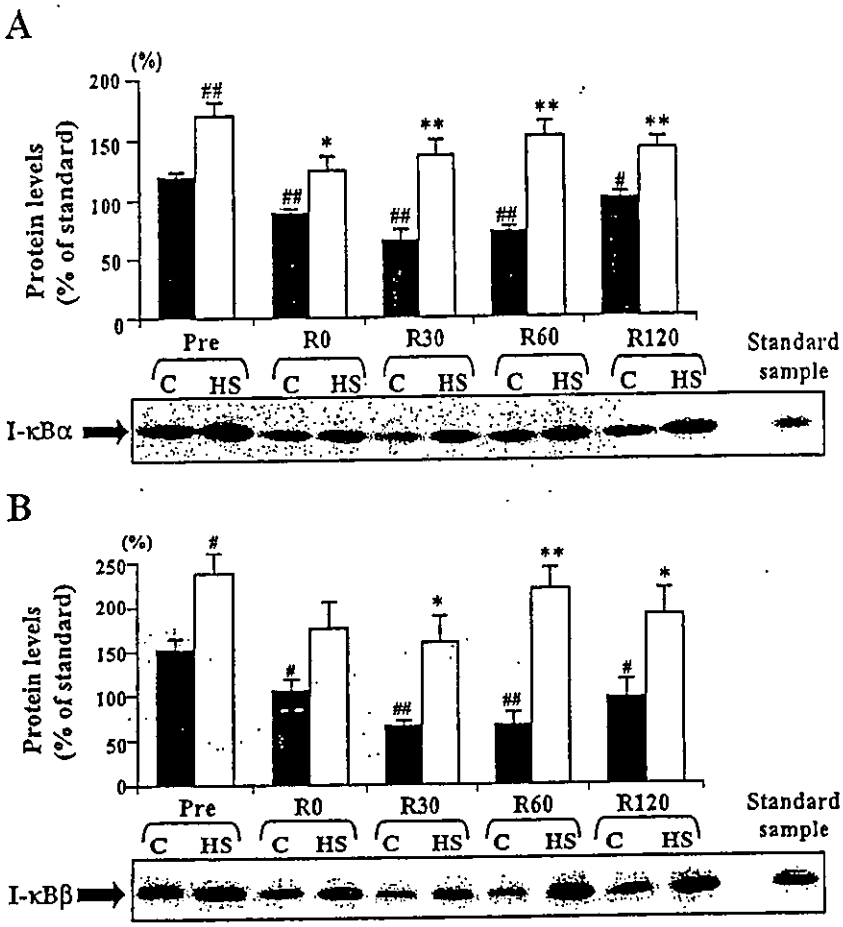

Fig. 4. The NF-κB inhibitor I-κB family protein levels in cytoplasm were analyzed using Western blotting analysis. The levels of I-κBα (*A*) and I-κBβ expression (*B*) during ischemia-reperfusion were examined in each group. Cytoplasmic extracts were prepared from liver samples obtained at the preischemic phase (48 h after preconditioning) and at 0, 30, 60, and 120 min postreperfusion. The standard sample was a cytoplasmic extract from a normal rat liver. The expression levels were evaluated on the same film as the ratio of their integrated intensity to that of the normal liver and presented as a percentage. Results are expressed as the means ± SE (n = 5 for each time point in each group). #$P < 0.05$ and ##$P < 0.01$ vs. Pre-C. *$P < 0.05$ and **$P < 0.01$ vs. *group C*. C, *group C*; HS, *group HS*; Pre-C, before ischemia in *group C*.

followed by the degradation of either I-κBα or I-κBβ. Neither could we, in the present study, detect serine phosphorylation of I-κB with Western blot analysis using anti-phospho-I-κB antibody (data not shown). However, degradation of I-κBα and I-κBβ occurred during the reperfusion phase despite the loss of serine phosphrylation. In addition, this degradation was not dependent on IKK activation. Although at this time, we cannot explain the discrepancies between our results and theirs, these results suggest the complexity of the activation pathways of NF-κB during I/R of the liver. It might be different from the generally accepted major pathways demonstrated in studies using proinflammatory mediators (36, 61). Many intracellular events (production of ROS, ATP depletion, intracellular Ca^{2+} accumulation, and activation of proteases) occur during hepatic I/R (20, 21, 33, 41, 66), and all of them can correlate with NF-κB activation through dif-

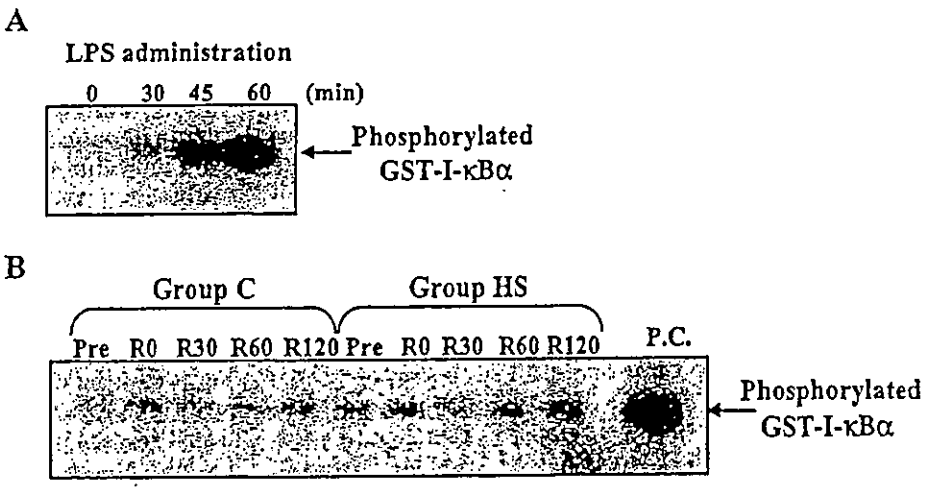

Fig. 5. The I-κB kinase (IKK) complex was immunoprecipitated using anti-NF-κB essential modulator antibody from liver tissue, and its activity was measured with an immunocomplex kinase assay using glutathione S-transferase-I-κBα (GST-I-κB). *A*: IKK activity in the liver tissue at 0, 30, 45, and 60 min after lipopolysaccharide (LPS) injection (2 mg/kg) was examined for the control of assay quality. IKK activity was very low in normal liver but dramatically increased after LPS injection in a time-dependent manner. *B*: activity of the IKK complex during hepatic ischemia-reperfusion. There were no increases in IKK activity in the liver during ischemia-reperfusion in either group. The figure shown is representative of 3 independent experiments.

ferent mechanism. In particular, the activation of proteases such as calpain, caspase, and lysosomal enzymes has been demonstrated to degrade I-κB without requiring IKK activation (11, 48). The COOH-terminal region of I-κB has signal sequences for protein instability (PEST sequences) (3, 50), which might be sensitive to degradation by these proteases. Therefore, it is likely that in our model, some proteolitic pathways may be involved in this IKK-independent I-κB degradation. However, further studies are necessary to evaluate this possibility.

With regard to the inhibition of NF-κB activation with HS preconditioning, our data revealed two possible mechanisms. The first mechanism is the increase in cytoplasmic I-κB proteins 48 h after HS preconditioning. Because the amount of cytoplasmic p65 was not increased by HS preconditioning, the increased I-κBs after HS preconditioning is probably free I-κB, which can interfere with the translocation of activated NF-κB. Many reports have demonstrated that increased I-κB expression decreases NF-κB activation (1, 46, 57). In addition, Pritts et al. (42) and Wong et al. (55, 56) demonstrated that the induction of the stress response increased I-κBα gene expression in vitro and in vivo. That is, I-κBα may be regarded as a stress protein. Further investigation is needed to determine whether an increased I-κB expression level with HS preconditioning is due to increased gene transcription, RNA stability, translation rate, or protein stability.

The other important mechanism showed how HS preconditioning maintained cytoplasmic I-κB protein levels similar to those of the control levels during hepatic I/R. Although HS preconditioning did not completely prevent decreases in I-κB levels, it blunted the consistent loss of I-κB proteins in the cytoplasm. These results are in agreement with the findings of several studies that have demonstrated that the stress response can inhibit I-κB degradation caused by various stimuli (13, 19, 43, 55, 63). Induction of a stress response in our study has been monitored in the liver by determining the maximum expression of HSP-72. It has been reported in some studies that this inhibition of I-κB degradation is provided by blocking IKK activation (13, 43, 63). But IKK was not activated in our model. As another inhibitory mechanism of I-κB degradation, the chaperoning function of HSP-72 may provide a clue. It is very likely that HSP-72 senses some conformational changes of I-κB proteins in its role as a molecular chaperone and during hepatic I/R interacts with modified I-κB to prevent the subsequent degradation or disassociation from NF-κB. This possibility is supported by studies showing that HSP-70 has the ability to bind with I-κB proteins using its chaperoning function (11, 24). However, a trial to demonstrate the specific binding of HSP-72 with NF-κB/I-κB complex using the immunoprecipitation method was unsuccessful. Inclusion of I-κBs or p65 was not detected in the immunoprecipitates from mouse monoclonal anti-HSP-72 antibodies (SPA-810; StressGen). Of course, these results do not preclude the binding of these molecules. It is possible that the site where HSP-72 binds to NF-κB/I-κB complex is located very close to the site where SPA-810 recognizes HSP-72, therefore preventing SPA-810 from recognizing the HSP-72 associated with the NF-κB/I-κB complex. We also intended to examine immunoprecipitation using polyclonal anti-I-κB or anti-p65 antibody from rabbits; but normal rabbit IgG (negative control) coimmunoprecipitated HSP-72 by itself. Further studies are needed to fully investigate potential mechanisms with which the stress response maintains cytoplasmic I-κB protein levels.

A recent report illustrated that the overexpression of Bcl-2 inhibited NF-κB activation by forming a stable complex with NF-κB components (27). Similar to HSP-72, Bcl-2 is known to be upregulated by HS (28). I-κB may also be inducible by stresses as described above. It is possible that these stress-inducible molecules might interact with and stabilize each other to achieve their cytoprotective functions. This hypothesis leads us to speculate on the existence of other molecules induced by HS preconditioning. These molecules might also participate in an interaction between NF-κB/I-κB complex and HSP-72.

In summary, we have shown that HS preconditioning inhibits hepatic I/R-induced NF-κB activation in vivo by affecting I-κB protein expression. This can be one of the mechanisms by which HS preconditioning reduces subsequent I/R damage to the liver. A better understanding of the role of the stress response in modifying the proinflammatory mediator cascade will contribute to the clinical application of HS preconditioning in reducing liver damage during I/R as well as for treating other diseases. It may also provide an important benchmark for exploring other chemicals or drugs that may supplant the effects of the stress response.

The authors thank D. A. Brenner, (Dept. of Medicine, Univ. of North Carolina at Chapel Hill) for valuable advice during this study.

This work was partly supported by a Grant-in-Aid of the Japan Society for the Promotion of Science, Tokyo Japan (Nos. 12470258 and 13557105).

REFERENCES

1. **Auphan N, DiDonato JA, Rosette C, Helmberg A, and Karin M.** Immunosuppression by glucocorticoids: inhibition of NF-κB activity through induction of I-κB synthesis. *Science* 270: 286–290, 1995.
2. **Baldwin AS Jr.** The NF-κ B and I κ B proteins: new discoveries and insights. *Annu Rev Immunol* 14: 649–83, 1996.
3. **Beauparlant P, Lin R, and Hiscott J.** The role of the C-terminal domain of I-κBα in protein degradation and stabilization. *J Biol Chem* 271: 10690–10696, 1996.
4. **Brecht M, Brecht C, and De Groot H.** Late steady increase in cytosolic Ca^{2+} preceding hypoxic injury in hepatocytes. *Biochem J* 283: 399–402, 1992.
5. **Burel C, Mezger V, Pinto M, Rallu M, Trigon S, and Morange M.** Mammalian heat shock protein families. *Expression and Functions Experientia* 48: 629–634, 1992.
6. **Colletti LM, Cortis A, Lukacs N, Kunkel SL, Green M, and Strieter RM.** Tumor necrosis factor up-regulates intercellular adhesion molecule 1, which is important in the neutrophil-dependent lung and liver injury associated with hepatic ischemia and reperfusion in the rat. *Shock* 10: 182–191, 1998.
7. **Colletti LM, Kunkel SL, Walz A, Burdick MD, Kunkel RG, Wilke CA, and Strieter RM.** Chemokine expression during

hepatic ischemia/reperfusion-induced lung injury in the rat. The role of epithelial neutrophil activating protein. *J Clin Invest* 95: 134–141, 1995.
8. **Colletti LM, Remick DG, Burtch GD, Kunkel SL, Strieter RM, and Campbell DA Jr.** Role of tumor necrosis factor-alpha in the pathophysiologic alterations after hepatic ischemia/reperfusion injury in the rat. *J Clin Invest* 85: 1936–1943, 1990.
9. **Collins T, Read MA, Neish AS, Whitley MZ, Thanos D, and Maniatis T.** Transcriptional regulation of endothelial cell adhesion molecules: NF-κB and cytokine-inducible enhancers. *FASEB J* 9: 899–909, 1995.
10. **Craig EA, Weissman JS, and Horwich AL.** Heat shock proteins and molecular chaperones: mediators of protein conformation and turnover in the cell. *Cell* 78: 365–372, 1994.
11. **Cuervo AM, Hu W, Lim B, and Dice JF.** IκB is a substrate for a selective pathway of lysosomal proteolysis. *Mol Biol Cell* 9: 1995–2010, 1998.
12. **Currie RW, Karmazyn M, Kloc M, and Mailer K.** Heat-shock response is associated with enhanced postischemic ventricular recovery. *Circ Res* 63: 543–549, 1988.
13. **Curry HA, Clemens RA, Shah S, Bradbury CM, Botero A, Goswami P, and Gius D.** Heat shock inhibits radiation-induced activation of NF-κB via inhibition of I-κB kinase. *J Biol Chem* 274: 23061–23067, 1999.
14. **DeMeester SL, Buchman TG, Qiu Y, Jacob AK, Dunnigan K, Hotchkiss RS, Karl I, and Cobb JP.** Heat shock induces IκB-alpha and prevents stress-induced endothelial cell apoptosis. *Arch Surg* 132: 1283–1288, 1997.
15. **De Vera ME, Kim YM, Wong HR, Wang Q, Billiar TR, and Geller DA.** Heat shock response inhibits cytokine-inducible nitric oxide synthase expression in rat hepatocytes. *Hepatology* 24: 1238–1245, 1996.
16. **Diaz-Guerra MJ, Velasco M, Martin-Sanz P, and Bosca L.** Nuclear factor κB is required for the transcriptional control of type II NO synthase in regenerating liver. *Biochem J* 326: 791–797, 1997.
17. **Drugas GT, Paidas CN, Yahanda AM, Ferguson D, and Clemens MG.** Conjugated desferoxamine attenuates hepatic microvascular injury following ischemia/reperfusion. *Circ Shock* 34: 278–283, 1991.
18. **Farhood A, McGuire GM, Manning AM, Miyasaka M, Smith CW, and Jaeschke H.** Intercellular adhesion molecule 1 (ICAM-1) expression and its role in neutrophil-induced ischemia-reperfusion injury in rat liver. *J Leukoc Biol* 57: 368–374, 1995.
19. **Feinstein DL, Galea E, Aquino DA, Li GC, Xu H, and Reis DJ.** Heat shock protein 70 suppresses astroglial-inducible nitric-oxide synthase expression by decreasing NF-κB activation. *J Biol Chem* 271: 17724–17732, 1996.
20. **Ferguson DM, Gores GJ, Bronk SF, and Krom RA.** An increase in cytosolic protease activity during liver preservation. Inhibition by glutathione and glycine. *Transplantation* 55: 627–633, 1993.
21. **Gasbarrini A, Borle AB, Farghali H, Bender C, Francavilla A, and Van Thiel D.** Effect of anoxia on intracellular ATP, Na^+_i, Ca^{2+}_i, Mg^{2+}_i, and cytotoxicity in rat hepatocytes. *J Biol Chem* 267: 6654–6663, 1992.
22. **Gerbes AL, Vollmar AM, Kiemer AK, and Bilzer M.** The guanylate cyclase-coupled natriuretic peptide receptor: a new target for prevention of cold ischemia-reperfusion damage of the rat liver. *Hepatology* 28: 1309–1917, 1998.
23. **Gething MJ and Sambrook J.** Protein folding in the cell. *Nature* 355: 33–45, 1992.
24. **Guzhova IV, Darieva ZA, Melo AR, and Margulis BA.** Major stress protein Hsp70 interacts with NF-kB regulatory complex in human T-lymphoma cells. *Cell Stress Chaperones* 2: 132–139, 1997.
25. **Hartl FU.** Molecular chaperones in cellular protein folding. *Nature* 381: 571–579, 1996.
26. **Hoshida S, Kuzuya T, Fuji H, Yamashita N, Oe H, Hori M, Suzuki K, Taniguchi N, and Tada M.** Sublethal ischemia alters myocardial antioxidant activity in canine heart. *Am J Physiol Heart Circ Physiol* 264: H33–H39, 1993.
27. **Hour TC, Chen L, and Lin JK.** Suppression of transcription factor NF-kB activity by Bcl-2 protein in NIH3T3 cells: implication of a novel NF-kB p50-Bcl-2 complex for the anti-apoptotic function of Bcl-2. *Eur J Cell Biol* 79: 121–129, 2000.
28. **Inoue Y, Sato Y, Nishimura M, Seguchi M, Zaitsu Y, Yamada K, and Oka Y.** Heat-induced drug resistance is associated with increased expression of Bcl-2 in HL60. *Anticancer Res* 19: 3989–3992, 1999.
29. **Jaeschke H and Farhood A.** Neutrophil and Kupffer cell-induced oxidant stress and ischemia-reperfusion injury in rat liver. *Am J Physiol Gastrointest Liver Physiol* 260: G355–G362, 1991.
30. **Jones BE, Lo CR, Liu H, Pradhan Z, Garcia L, Srinivasan A, Valentino KL, and Czaja MJ.** Role of caspases and NF-κB signaling in hydrogen peroxide- and superoxide-induced hepatocyte apoptosis. *Am J Physiol Gastrointest Liver Physiol* 278: G693–G699, 2000.
31. **Kimoto S, Yamamoto Y, Yamagami K, Ishikawa Y, Kume M, Yamamoto H, Ozaki N, and Yamaoka Y.** The augmentative effect of repeated heat shock preconditioning on the production of heat shock protein 72 and on ischemic tolerance in rat liver tissue. *Int J Hyperthermia* 16: 247–261, 2000.
32. **Kinoshita T, Imamura J, Nagai H, and Shimotohno K.** Quantification of gene expression over a wide range by the polymerase chain reaction. *Anal Biochem* 206: 231–235, 1992.
33. **Kohli V, Madden JF, Bentley RC, and Clavien PA.** Calpain mediates ischemic injury of the liver through modulation of apoptosis and necrosis. *Gastroenterology* 116: 168–178, 1999.
34. **Lentsch AB, Yoshidome H, Cheadle WG, Miller FN, and Edwards MJ.** Chemokine involvement in hepatic ischemia/reperfusion injury in mice: roles for macrophage inflammatory protein-2 and KC. *Hepatology* 27: 1172–1177, 1998.
35. **Lindquist S and Craig EA.** The heat-shock proteins. *Annu Rev Genet* 22: 631–677, 1988.
36. **Mercurio F, Zhu H, Murray BW, Shevchenko A, Bennett BL, Li J, Young DB, Barbosa M, Mann M, Manning A, and Rao A.** IKK-1 and IKK-2: cytokine-activated I-κB kinases essential for NF-κB activation. *Science* 278: 860–866, 1997.
37. **Minowada G and Welch WJ.** Clinical implications of the stress response. *J Clin Invest* 95: 3–12, 1995.
38. **Mizushima Y, Wang P, Jarrar D, Cioffi WG, Bland KI, and Chaudry IH.** Preinduction of heat shock proteins protects cardiac and hepatic functions following trauma and hemorrhage. *Am J Physiol Regulatory Integrative Comp Physiol* 278: R352–R359, 2000.
39. **Morimoto RI and Santoro MG.** Stress-inducible responses and heat shock proteins: new pharmacologic targets for cytoprotection. *Nat Biotechnol* 16: 833–838, 1998.
40. **Morishita R, Sugimoto T, Aoki M, Kida I, Tomita N, Moriguchi A, Maeda K, Sawa Y, Kaneda Y, Higaki J, and Ogihara T.** In vivo transfection of *cis* element against nuclear factor-κB binding site prevents myocardial infarction. *Nat Med* 3: 894–899, 1997.
41. **Ozaki M, Deshpande SS, Angkeow P, Bellan J, Lowenstein CJ, Dinauer MC, Goldschmidt-Clermont PJ, and Irani K.** Inhibition of the Rac1 GTPase protects against nonlethal ischemia/reperfusion-induced necrosis and apoptosis in vivo. *FASEB J* 14: 418–429, 2000.
42. **Pritts TA, Wang Q, Sun X, Moon MR, Fischer DR, Fischer JE, Wong HR, and Hasselgren PO.** Induction of the stress response in vivo decreases nuclear factor-κB activity in jejunal mucosa of endotoxemic mice. *Arch Surg* 135: 860–866, 2000.
43. **Roussel RR and Barchowsky A.** Arsenic inhibits NF-κB-mediated gene transcription by blocking I-κB kinase activity and I-κBα phosphorylation and degradation. *Arch Biochem Biophys* 377: 204–212, 2000.
44. **Saad S, Kanai M, Awane M, Yamamoto Y, Morimoto T, Isselhard W, Minor T, Troidl H, Ozawa K, and Yamaoka Y.** Protective effect of heat shock pretreatment with heat shock protein induction before hepatic warm ischemic injury caused by Pringle's maneuver. *Surgery* 118: 510–516, 1995.
45. **Scarim AL, Heitmeier MR, and Corbett JA.** Heat shock inhibits cytokine-induced nitric oxide synthase expression by rat and human islets. *Endocrinology* 139: 5050–5057, 1998.

46. Scheinman RI, Cogswell PC, Lofquist AK, and Baldwin AS Jr. Role of transcriptional activation of I-κBα in mediation of immunosuppression by glucocorticoids. *Science* 270: 283–286, 1995.
47. Schneider A, Martin-Villalba A, Weih F, Vogel J, Wirth T, and Schwaninger M. NF-κB is activated and promotes cell death in focal cerebral ischemia. *Nat Med* 5: 554–559, 1999.
48. Schoonbroodt S, Ferreira V, Best-Belpomme M, Boelaert JR, Legrand-Poels S, Korner M, and Piette J. Crucial role of the amino-terminal tyrosine residue 42 and the carboxyl-terminal PEST domain of I-κB alpha in NF-κB activation by an oxidative stress. *J Immunol* 164: 4292–4300, 2000.
49. Schwabe RF, Bennett BL, Manning AM, and Brenner DA. Differential role of I-κB kinase 1 and 2 in primary rat hepatocytes. *Hepatology* 33: 81–90, 2001.
50. Shumway SD, Maki M, and Miyamoto S. The PEST domain of I-κBα is necessary and sufficient for in vitro degradation by mu-calpain. *J Biol Chem* 274: 30874–30881, 1999.
51. Stein B and Baldwin AS Jr. Distinct mechanisms for regulation of the interleukin-8 gene involve synergism and cooperativity between C/EBP and NF-κB. *Mol Cell Biol* 13: 7191–7198, 1993.
52. Welch WJ. Mammalian stress response: cell physiology, structure/function of stress proteins, and implications for medicine and disease. *Physiol Rev* 72: 1063–1081, 1992.
53. Widmer U, Manogue KR, Cerami A, and Sherry B. Genomic cloning and promoter analysis of macrophage inflammatory protein (MIP)-2, MIP-1 α, and MIP-1 β, members of the chemokine superfamily of proinflammatory cytokines. *J Immunol* 150: 4996–5012, 1993.
54. Wong HR, Ryan M, and Wispe JR. The heat shock response inhibits inducible nitric oxide synthase gene expression by blocking Iκ-B degradation and NF-κB nuclear translocation. *Biochem Biophys Res Commun* 231: 257–263, 1997.
55. Wong HR, Ryan M, and Wispe JR. Stress response decreases NF-κB nuclear translocation and increases I-κBα expression in A549 cells. *J Clin Invest* 99: 2423–2428, 1997.
56. Wong HR, Ryan MA, Menendez IY, and Wispe JR. Heat shock activates the I-κBalpha promoter and increases I-κBα mRNA expression. *Cell Stress Chaperones* 4: 1–7, 1999.
57. Wrighton CJ, Hofer-Warbinek R, Moll T, Eytner R, Bach FH, and de Martin R. Inhibition of endothelial cell activation by adenovirus-mediated expression of I-κBα, an inhibitor of the transcription factor NF-κB. *J Exp Med* 183: 1013–1022, 1996.
58. Xie QW, Kashiwabara Y, and Nathan C. Role of transcription factor NF-κB/Rel in induction of nitric oxide synthase. *J Biol Chem* 269: 4705–4708, 1994.
59. Yamagami K, Yamamoto Y, Ishikawa Y, Yonezawa K, Toyokuni S, and Yamaoka Y. Effects of geranyl-geranyl-acetone administration before heat shock preconditioning for conferring tolerance against ischemia-reperfusion injury in rat livers. *J Lab Clin Med* 135: 465–475, 2000.
60. Yamamoto Y, Kume M, and Yamaoka Y. Implications of heat shock proteins during liver surgery and liver perfusion. *Recent Results Cancer Res* 147: 157–172, 1998.
61. Yamaoka S, Courtois G, Bessia C, Whiteside ST, Weil R, Agou F, Kirk HE, Kay RJ, and Israel A. Complementation cloning of NEMO, a component of the IκB kinase complex essential for NF-κB activation. *Cell* 93: 1231–1240, 1998.
62. Yonezawa K, Yamamoto Y, Yamamoto H, Ishikawa Y, Uchinami H, Taura K, Nakajima A, and Yamaoka Y. Suppression of tumor necrosis factor-α production and neutrophil infiltration during ischemia-reperfusion injury of the liver after heat shock preconditioning. *J Hepatol* 35: 619–627, 2001.
63. Yoo CG, Lee S, Lee CT, Kim YW, Han SK, and Shim YS. Anti-inflammatory effect of heat shock protein induction is related to stabilization of I κ B alpha through preventing I-κB kinase activation in respiratory epithelial cells. *J Immunol* 164: 5416–5423, 2000.
64. Yoshidome H, Kato A, Edwards MJ, and Lentsch AB. Interleukin-10 suppresses hepatic ischemia/reperfusion injury in mice: implications of a central role for nuclear factor κB. *Hepatology* 30: 203–208, 1999.
65. Zwacka RM, Zhang Y, Zhou W, Halldorson J, and Engelhardt JF. Ischemia/reperfusion injury in the liver of BALB/c mice activates AP-1 and nuclear factor κB independently of IκB degradation. *Hepatology* 28: 1022–1030, 1998.
66. Zwacka RM, Zhou W, Zhang Y, Darby CJ, Dudus L, Halldorson J, Oberley L, and Engelhardt JF. Redox gene therapy for ischemia/reperfusion injury of the liver reduces AP1 and NF-κB activation. *Nat Med* 4: 698–704, 1998.

Free Radical Research, 2002 Vol. 36 (2), pp. 169–176

Taylor & Francis
healthsciences

Heat Shock Preconditioning Reduces the Formation of 8-hydroxy-2′-deoxyguanosine and 4-hydroxy-2-nonenal Modified Proteins in Ischemia-reperfused Liver of Rats

KAZUHIKO YAMAGAMI[a,b], YUZO YAMAMOTO[a,*], SHINYA TOYOKUNI[b], KOICHIRO HATA[a] and YOSHIO YAMAOKA[a]

[a]*Department of Gastroenterological Surgery, Kyoto University, Graduate School of Medicine, 54 Kawahara-cho, Shogoin, Sakyo-ku, Kyoto 606-8507, Japan;* [b]*Department of Pathology and Biology of Diseases, Kyoto University, Graduate School of Medicine, 54 Kawahara-cho, Shogoin, Sakyo-ku, Kyoto 606-8507, Japan*

Accepted by Professor E. Niki

(Received 22 June 2001; In revised form 5 September 2001)

Heat shock preconditioning (HSPC) is a promising strategy for providing ischemic tolerance. The objective of this study is to investigate the effectiveness of HSPC in preventing oxidative damage of cellular proteins and DNA during ischemia–reperfusion of the liver. Male Wistar rats were divided into a heat shock group (group HS) and control (group C). Forty-eight hours prior to ischemia, rats in group HS received HSPC at 42°C for 15 min. All rats received hepatic warm ischemia for 30 min and subsequent reperfusion. The formation of 8-hydroxy-2′-deoxyguanosine (8-OHdG), 4-hydroxy-2-nonenal (HNE) modified proteins in liver tissue, survival rate of the animals, and changes in biochemical and histological parameters were compared between groups. Heat shock protein 72 was produced only in group HS. The 7-day survival of rats was significantly better in group HS (10/10) than in group C (5/10) ($p < 0.01$). The serum release of alanine aminotransferase ($n = 10$, $p < 0.01$) and the concentration of adenosine triphosphate in liver tissue ($n = 10$, $p < 0.01$) 40 min after reperfusion was significantly better in group HS than in group C. The formation of 8-OHdG in liver tissue measured by high-performance liquid chromatography was suppressed in group HS ($p < 0.01$). The production of HNE-modified proteins as determined by Western-blot analysis was also decreased in group HS. These results were also confirmed by immunohistochemical analysis. As determined by levels of 8-OHdG and HNE-modified proteins produced during ischemia–reperfusion of the liver, HSPC reduced the oxidative injury of cellular proteins and DNA in the liver tissue.

Keywords: Heat shock protein 72; Ischemia–reperfusion injury; Liver; Reactive oxygen species; 8-Hydroxy-2′-deoxyguanosine; 4-Hydroxy-2-nonenal modified proteins

INTRODUCTION

Conditions resulting from ischemia–reperfusion (IR) occur during such surgical interventions as temporary total hepatic inflow clamping (Pringle's maneuver) or during the reconstruction of large vessels in liver surgery and liver transplantation. IR injury greatly impairs postischemic liver function and easily leads patients into postoperative liver failure. Although the exact mechanism of IR injury is still unclear, numerous reports in the last decade have shown that the uncontrolled production of reactive oxygen species (ROS) plays a significant role in the pathogenesis of IR injury of the liver.[1–3] The involvement of neutrophils in this process has been suggested.[4,5] To regulate intracellular ROS, cells develop various enzymatic and non-enzymatic defense systems. However, a certain fraction of ROS escapes cellular defenses and causes either permanent or transient damage to constitutive proteins, lipids, and nucleic acids,[6,7] resulting in cellular death.

Antioxidants and enzymes such as superoxide dismutase,[8–11] catalase,[12] and alpha-tocophenol[13] were reported to be protective against ROS injury during IR, however, it would be, difficult to utilize these antioxidants or enzymes clinically in their present form.

*Corresponding author. Tel.: +81-75-751-3241. Fax: +81-75-752-4519. E-mail: mai@kuhp.kyoto-u.ac.jp.

ISSN 1071-5762 print/ISSN 1029-2470 online © 2002 Taylor & Francis Ltd
DOI: 10.1080/10715760290006385

We reported the efficacy of heat shock preconditioning (HSPC), a new powerful strategy to evoke an endogenous protection response, which induced abundant heat shock protein 72 (HSP72) in normal, fibrotic, and steatotic rat livers.[14–16] Heat shock protein 72, a molecular chaperone, prevents denaturation and aggregation of proteins during stress and is recognized as a key protein in conferring stress tolerance.[17] ROS-induced DNA damage includes oxidative modification of bases as well as single and double strand breaks.[18] Among the modification of DNA bases, the formation of 8-hydroxy-2′-deoxyguanosine (8-OHdG) is one of the most commonly used markers for evaluating oxidative DNA damage. In our previous study, the level of 8-OHdG was quite useful for assessing DNA damage during IR injury in rat livers.[19] 4-Hydroxy-2-nonenal (HNE) is an alpha, beta-unsaturated aldehyde and one of the major components of lipid peroxidation products. It reacts with proteins to form HNE-modified proteins.[20,21] Since HNE-modified proteins are relatively stable, they can be used as a marker of ROS-mediated protein damage. We have shown that the formation of HNE-modified proteins is closely correlated with liver damage due to IR injury,[16,19,22] and suggests that two major proteins with molecular weights of 31 and 42 kDa are key targets for IR injury in rat livers.[19]

In this study, we investigated the effect of HSPC in light of oxidative DNA damage and cellular protein denaturation during IR of the liver by evaluating the formation of 8-OHdG and HNE-modified proteins, respectively.

MATERIALS AND METHODS

Animals

This study was conducted in compliance with the Animal Protection Guidelines of Kyoto University and all rats were treated humanely. Specific pathogen-free male Wistar rats (Shizuoka Laboratory Animal Center: Shizuoka, Japan), weighing between 230 and 260 g and between 10 and 11 weeks of age, were housed in an air conditioned room (24 ± 1°C) with alternating 12 h light and dark cycles, and were fed with a standard animal diet.

Study Protocol

A total of 76 rats were used. All surgical procedures were performed under general anesthesia with intraperitoneal injection of sodium pentobarbital (40 mg/kg) in an operating room temperature-controlled for these animals (24 ± 1°C). The animals were divided into two groups: A heat shock preconditioning group (group HS) and a control group (group C). Rats in group HS were placed in a temperature-controlled water bath to keep their rectal temperature at 42°C for 15 min. Rats in group C were temperature-controlled at 37°C instead of 42°C. Forty-eight hours after this pretreatment, the livers of rats in both groups were exposed to a 30 min warm ischemic insult by clamping inflow vessels. This was followed by a 40 min *in situ* reperfusion.

Using a steel tongue pre-cooled with liquid nitrogen, shock-frozen liver samples from the left lateral lobes were obtained before ischemia ($n = 7$), after ischemia ($n = 10$) and 40 min after reperfusion ($n = 10$). At these same time intervals, liver samples from the right lobes were also obtained for histological examination. Aortic blood samples were collected 40 min after reperfusion ($n = 10$).

Measurement of Liver Related Enzymes, Energy Metabolism, and Survival Rate

Alanine aminotransferase (ALT) was measured in a biochemical laboratory. Concentration of adenine nucleotides in liver tissues was assayed enzymatically.[23,24] Survival rate was determined on post-operative day 7.

Analysis of 8-OHdG

DNA was extracted from the frozen samples by the NaI method with minor modifications (DNA extractor WB kit: Wako, Osaka, Japan).[25] DNA was digested with nuclease P1 (Sigma: St. Louis, MO, USA) and alkaline phosphatase (Boehringer Mannheim: Tokyo, Japan). As previously described,[26] the production of 8-OHdG was then analyzed from the DNA extracts using high performance liquid chromatography (HPLC) and an electrochemical detector (Coulochem II, ESA: Bedfold, MA, USA).

Immunohistochemical Analysis

After samples were fixed with Bouin's solution,[27] immunohistochemical staining of HSP72 (anti-HSP72 antibody: SPA-810; StressGen Biotechnologies, Victoria, British Columbia, Canada), 8-OHdG,[26] and HNE-modified proteins[28] was performed using the ABC method in conjunction with alkaline phosphatase. In order to achieve high sensitivity, black substrate (Vector Laboratories: Burlingame, CA, USA) was used as the final detection reagent.

Western Blotting Analysis

Frozen samples (weighing approximately 40 mg) were homogenized in a lysis buffer. The suspensions for HSP72 and HNE-modified proteins were centrifuged at 15,000*g* for 15 min and 105,000*g* for

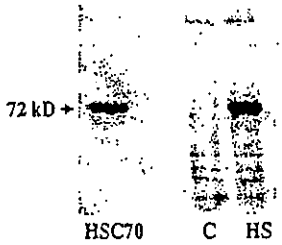

FIGURE 1 Western blotting analysis of HSP72 production in livers 48 h after reperfusion C: control; HS: group HS. Protein concentrations are 3 μg/lane in the samples and 0.2 μg/lane in the positive control (HSC70).

60 min, respectively, at 4°C. Protein concentration was determined using a BCA protein assay kit (Pierce: Rockford, IL, USA). Samples were run onto a 10% (HSP72) or a 12.5% (HNE-modified proteins) polyacrylamide gel with 0.1% sodium dodecyl sulfate and were used for Western blot analysis as previously described.[19,29] Finally, they were reacted with enhanced chemiluminescence detection reagent (Amersham International: Buckinghamshire, England) and the results were visualized on X-ray (Hyper film ECL: Amersham). Densitometric analysis was performed with a GS-700 Imaging Densitometer (Bio-Rad Laboratories: CA, USA).

Statistical Analysis

Data are shown as means ± SD. One way analysis of variance and an unpaired *t*-test were used to analyze the changes in metabolic parameters. A chi-square test was used for survival rate. *p*-Values less than 0.05 were considered statistically significant.

RESULTS

Detection of HSP72

Figure 1 shows the amount of HSP72 in liver tissue 48 h after HSPC. Heat shock protein 72 was strongly expressed in group HS, while a band of HSP72 was not detected in group C. Figure 2 shows immunohistochemical staining of HSP72 in liver tissue. The control liver was not stained, but HSP72-positive hepatocytes were distributed in pericentral and periportal liver tissue after HSPC. The nuclei as well as the cytoplasm of hepatocytes were stained with a specific anti-HSP72 antibody.

Animal Survival, Liver Related Enzymes and Energy Metabolism

Seven-day survival of the rats, as well as their serum levels of ALT and their ATP concentrations in liver tissue after warm ischemic insult is presented in Table I. While all the animals survived (10/10) in group HS, only 50% (5/10) survived in group C ($p < 0.01$). Forty minutes after reperfusion, levels of ALT in group HS were significantly lower than levels in group C ($p < 0.01$). In addition, during the 40 min after reperfusion, there was a better recovery of ATP concentrations in liver tissue in group HS than in group C ($p < 0.01$).

8-OHdG Level in the Liver Tissue After IR Injury

Tissue levels of 8-OHdG are summarized on Table II. In group C, there was a 2.4-fold increase in 8-OHdG levels during ischemia and a further increase to 6.1-fold during reperfusion. In group HS, the increase in 8-OHdG during ischemia was not different from the increase seen in group C, but the increase during reperfusion was significantly less than the levels in group C ($p < 0.01$).

HNE-modified Proteins in the Liver After IR Injury

Several bands of HNE-modified proteins were detected by Western blotting analysis (Fig. 3A). Two major bands were located at 42 and 31 kDa

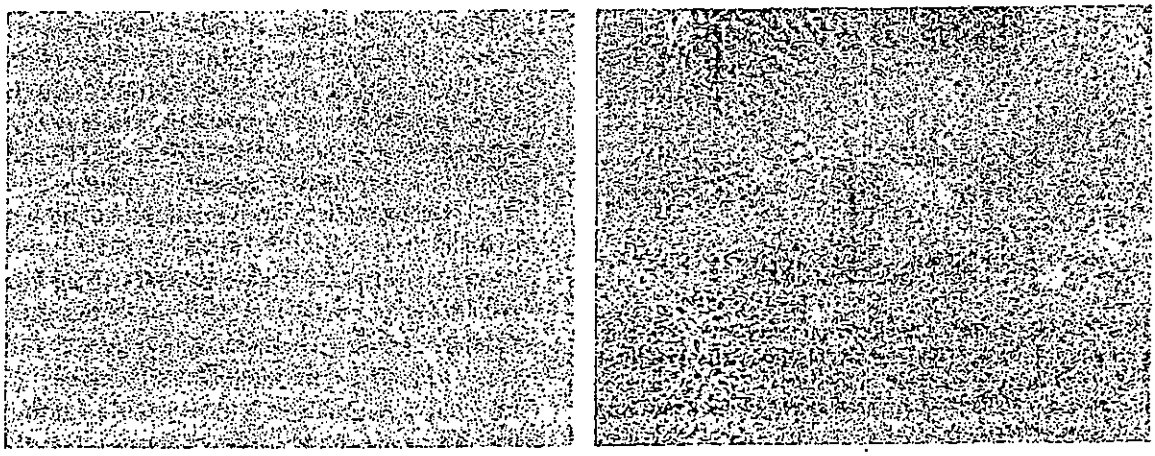

FIGURE 2 Immunohistochemical analysis of HSP72. (A) Control rat livers. (B) Rat livers 48 h after heat shock preconditioning (Original magnification × 10).

TABLE I

Survival rate on POD 7	
Group C	5/10 (50%)
Group HS	10/10 (100%)*
Serum ALT levels 40 min after reperfusion	
Group C	1349 ± 240
Group HS	699 ± 160*
ATP concentration in liver tissue 40 min after reperfusion	
Group C	0.759 ± 0.277
Group HS	1.680 ± 0.244*

C: control; HS: heat shock; POD: postoperative day.
Data are expressed as mean ± SD, $n = 10$, $*p < 0.01$ vs. control.

after reperfusion in both groups. Although these two bands were visible even in untreated group reflecting the baseline lipid peroxidation in the normal liver tissue, they were prominently strong in group C and depressed in group HS. Densitometric analysis demonstrated that the intensity of these two major bands was lower in group HS than in group C (Fig. 3B).

Immunohistochemical Staining of 8-OHdG and HNE-modified Proteins

Figure 4 illustrates hematoxylin and eosin staining of the liver tissue after reperfusion. In group C, severe congestion as well as massive necrotic areas were noted, but these damages were markedly less in group HS. Both 8-OHdG and HNE-modified proteins were faintly stained in livers before IR in group C and in group HS. After IR, 8-OHdG

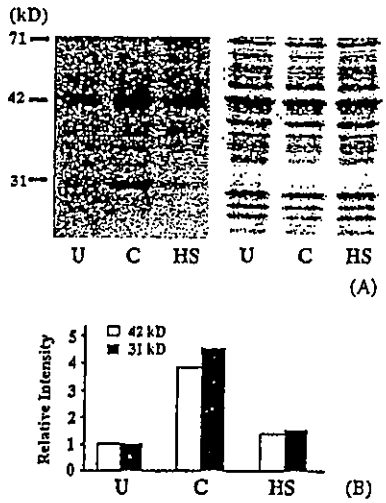

FIGURE 3 HNE-modified proteins in livers after ischemia-reperfusion injury. (A) Western blotting analysis (Protein concentrations are 20 μg/lane in the sample). Two major bands were located at 42 and 31 kDa. The intensity of these two major bands was lower in group HS than in group C. Coomassie brilliant blue staining of the gel shows the equal amount of proteins applied on each lane. (B) Densitometoric analysis of 42 and 31 kDa proteins. U: untreated liver; C: control; HS: group HS.

TABLE II 8-OHdG levels after warm ischemia and reperfusion

Treatment	8-OHdG/10^5 × dG
Before clamping ($n = 7$)	
Control	0.70 ± 0.32
HS	0.83 ± 0.24
End of ischemia ($n = 10$)	
Control	1.68 ± 0.27
HS	1.50 ± 0.34
Reperfusion (40 min) ($n = 10$)	
Control	4.24 ± 0.90
HS	2.95 ± 0.60*

HS: heat shock.
Data are expressed as mean ± SD, $*p < 0.01$ vs. control.

immunostaining was intense in the nuclei of cells in group C. However, the nuclear staining in group HS was significantly less modified than in group C (Fig. 5). In a similar way, HNE-modified proteins were strongly immunostained after IR in the cytoplasm of hepatocytes in group C except in necrotic areas. On the other hand, staining in group HS was significantly suppressed (Fig. 6).

DISCUSSION

Our prior experiments have demonstrated that HSPC or concomitantly induced HSP72 provided livers with tolerance against IR injury.[14–16] The beneficial effects of HSP72 on IR injury were also reported in other organs including the heart and lungs.[30,31] But the cytoprotective mechanism of HSPC against IR injury has not been clearly defined. Our present data show that the formation of oxidative-damage products (8-OHdG and HNE-modified proteins) was significantly decreased in group HS. That is, HSPC reduced the oxidative damage of DNA in nuclei and of proteins in cytosol. Decreased formation of these unfavorable products in hepatocytes after lethal ischemia in group HS is consistent with better animal survival, less release of liver-related enzymes and more rapid recovery of hepatic energy metabolism.

Membrane lipids are the first targets of ROS attacks. The final products of lipid peroxidation are mostly aldehydes. HNE, one of these aldehydes, has high reactivity with cytosolic proteins. We have demonstrated that the formation of HNE-modified proteins is a sensitive marker for evaluating levels of lipid peroxidation and oxidative denaturation of cytosolic proteins.[32] Identification of two major proteins—42 and 31 kDa—was effective for assessing the IR injury of rat livers.[19] Concerning these two proteins, further characterization is of great importance to clarify the detailed mechanism, but the molecular weights do not provide enough information to estimate the candidate proteins. Proteins having histidine-, cystein- or lysine-residue, which easily reacts with HNE, on their outer surface, will be